Construction and Building Materials 218 (2019) 8–27

Contents lists available at ScienceDirect

Construction and Building Materials

journal homepage: www.elsevier.com/locate/conbuildmat

Effect of porosity on predicting compressive and flexural strength of cement mortar containing micro and nano-silica by ANN and GEP

Seyed Ali Emamian, Hamid Eskandari-Naddaf *

Department of Civil Engineering, Hakim Sabzevari University, Sabzevar, Iran

HIGHLIGHTS

- The effect of porosity on macro and microstructures of cement mortar is examined.
- ANN and GEP are the powerful tools to predict the strength of the cement mortar.
- There is a good correlation between experimental, ANN, and GEP results.
- The performance of ANN and GEP models is improved by considering porosity.

GRAPHICAL ABSTRACT

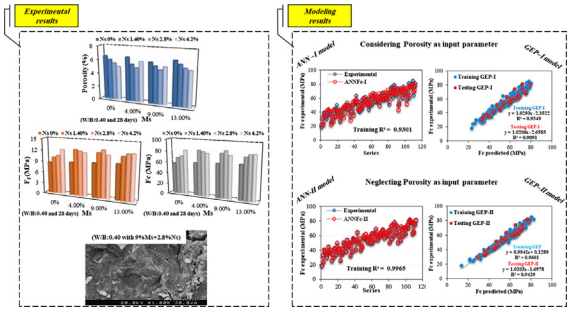

ARTICLE INFO

Article history:
Received 26 June 2018
Received in revised form 23 April 2019
Accepted 13 May 2019

Keywords:
Cement mortar
Nano and micro silica
Porosity
Mechanical properties
Microstructure analysis
Artificial neural network
Genetic expression program

ABSTRACT

The aim of this study is to evaluate the effect of porosity on mechanical properties of cement mortar containing micro and nano silica in two aspects of experimentation and modeling of prediction. For this purpose, 32 mix designs were considered with various replacement percentages of nano silica (Ns) and micro silica (Ms) in forms of alone and together. The microstructure effect of Ns and Ms on the mechanical properties of cement mortar was investigated by Field Emission Scanning Electron Microscopy (FE-SEM) analysis. Moreover, Artificial Neural Network (ANN) and Genetic Expression Program (GEP) models are presented to predict the compressive and flexural strengths of cement mortar by focusing on the effect of porosity in models. So, a comparative probe was carried out on two statuses. Once, porosity wasn't considered as input parameter, and, in the next step, it was considered as input parameter in developing ANN-I or GEP-I and ANN-II or GEP-II models, respectively, in order to specify the sensitivity of the models to select the proper input parameters for accurate prediction. The results showed that the use of simultaneous Ns and Ms led to a decrease in the porosity and an increase in the flexural and compressive strengths. This is due to the synergistic effect on the microstructure of cement paste. The current modeling results showed that the ANN-II and GEP-II models have higher accuracy in the prediction of mechanical properties considering porosity as an influential input parameter. Moreover, the validation of proposed models was evaluated with the help of a collection of previous literature.

1. Introduction

Cement mortar is a basic cementitious material with a composite structure that, creates diverse properties by utilizing various admixtures [1–3]. Therefore, mechanical properties of cement mortars are not dependent on one parameter alone but under the influence of the relationship among several parameters such as water to cement ratio (W/C) [4], aggregate to cement ratio (Agg/C) [5,6], age [7,8], and admixture [9,10] of specimens. For instance, previous studies by Kim et al. [11] and Eskandari et al. [12] investigated the effect of W/C and aggregate grading on

* Corresponding author.
E-mail addresses: s.ali.emamian@gmail.com (S.A. Emamian), Hamidiisc@yahoo.com, h.eskandari@hsu.ac.ir (H. Eskandari-Naddaf).

https://doi.org/10.1016/j.conbuildmat.2019.05.092
0950-0618/

mechanical properties of cement mortar, so that their results showed that reduction of W/C and size of the aggregate particles lead to the increase of compressive strength of cementitious materials. Nowadays, there are so many admixture materials to improve physical and mechanical properties of cementitious materials, while the pozzolanic materials can substitute cement in the mortar and concrete [13–15]. The pozzolanic materials like nano silica (Ns) or micro silica (Ms) are the effective components in the quality of cement mortar which can make a unique performance in terms of strength, permeability, corrosion, resistance, and durability [16–18]. There are two important reasons for using Ns and Ms: a filler role due to small particle size and the pozzolanic reaction with $Ca(OH)_2$ in the cement mortar hydration process [19]. Hence, cementitious materials properties can be affected by the amount of Ns and Ms, so that determining their optimal percentage is still under discussion [20,21].

On the other hand, size, volume, and distribution of pores are efficient parameters in the macrostructure level which influence the mechanical properties and porosity. The significant issue in the investigated macro analysis is considering the accurate parameter in the basic constituent of cementitious materials and cementitious replacement materials in mortar mixtures. In addition, the microstructure study provides more details about internal structures and, following that, changes in macro-level properties. Meanwhile, many studies have been done to investigate the relationship between porosity and pore size distribution on mechanical and microstructural properties. For example, the effect of microstructural characteristics of nano-particles has been evaluated in the compressive and flexural strengths of cement mortar, and the results have been shown the supreme mechanical performance of nano-particles through filling up the pores and activator role to promote hydration products [22]. Li et al. [20] evaluated the effect of Ms and Ns in the filling void to increase the density of the cementitious materials in order to improve the microstructure. In another study, Ozturk and Baradan [23] have investigated the relationship between microstructure effects such as pore structure and pore size distribution on cement strength properties. On the other hand, due to the well-known relationship between porosity and mechanical properties of cement mortar, porosity evaluation is a priority in evaluating the properties of cementitious materials.

In recent years, the use of intelligence tools has been developed in civil engineering problems [24,25], and Artificial Neural Network (ANN) and Genetic Expression Program (GEP) are strong prediction models among these [15]. These models are more popular and efficient for complex problems due to classifying data and learning the input and output data relation [26,27]. The prediction of mechanical properties of mortar which have been made with different mix designs depends on selecting suitable parameters in order to achieve the acceptable model. In this regard, several reports were published that show the use of ANN and GEP for predicting the compressive and flexural strengths of cement mortar [28,29]. Even though these previous reports typically have had acceptable results in predicting by their proposed models, some of their models have indicated large errors in the performance of their predictions. For instance, Yuan et al. [30] and Gupta [31] predicted compressive strength of concrete which is containing admixture for data that was gathered from previous literature by ANN and GA-ANN for compressive strength specimens at age of 28 days. Their results show that some results did not fit well, and large errors may occur which are related to not considering the input parameters in their proper form. It is known that the mechanical properties such as compressive and flexural strengths depend on water to cement ratio, aggregate to cement ratio, and alternative additives to cement ratio, while in these studies parameters are separately presented and weighted. Moreover, due to the above mentioned reasons, regarding the effect of porosity on mechanical properties has considered in none of these predicted models as an input parameter.

The present study is focused on porosity effect of macro and microstructure properties of cement mortar containing Ns and Ms with different replacement percentages on compressive and flexural strengths. In addition, ANN and GEP models have been employed in two different states (with and without considering porosity as input parameter) in identifying the performance change in proposed models. Finally, the proposed models are verified with the help of collected data from the previous literature.

2. Experimental plan

2.1. Materials

The Portland cement with the grade of 52.5 MPa was used in this study. Ms and Ns were replaced as supplementary cementitious materials in mix designs with different percentages of 0%, 4%, 9%, 13% and 0%, 1.4%, 2.8% and 4.2%, respectively. The summaries of chemical and physical properties of cement, Ms and Ns, are presented in Table 1. The size distribution of sand was in accordance with ASTM C778 [32], and the maximum dimension of sand was equal to 4.75 mm.

2.2. Mix design, sample preparation, and testing

The used cement mortar contains Ns and Ms with 32 different mix designs. Each mix design consists of cement (C), sand (S), and binder (C + Ns + Ms); the details of all 32 mix proportions are listed in Table 2. Also, the various values of Ms and Ns as the partial cement replacement are applied in the cement mixture lead to achieving the optimal range of Ns and Ms values according to the previous literature [13,14]. The specimens which have been employed for compressive and flexural strength test are the cubes specimens with a dimension of $50 \times 50 \times 50\ mm^3$ and the prismatic specimens with dimensions of $40 \times 40 \times 160\ mm^3$,respectively. The cubes and prisms are immersed in the water tank at $25 \pm 1\ ^\circ C$ till time of testing. It is worth noting that cubes and prisms are de-molded after 24 h curing in the molds, then the specimens are cured in a water tank for 3, 7, 14, 21 and 28 days. The number of compressive and flexural tested specimens are 480 and 96, respectively, while the reported values are average of three specimens for each mix design. The porosity is obtained based on the weight variation of specimens on each age's dataset (3, 7, 14, 21 and 28 days). At first, the specimens were placed in an oven at $105 \pm 5\ ^\circ C$ to reach the stable weight (W_d). Then, the weight of

Table 1
Properties of Portland cement, micro silica and nano silica.

cementations materials	Chemical Analysis (wt %)												Physical Analysis	
	SiO_2	Al_2O_3	Fe_2O_3	CaO	MgO	SO_3	Na_2O	K_2O	LOI	F.CaO	C_3A	C_3S	Specific Gravity (ton/m^3)	Blaine Test (cm^2/gr)
C 52.5	21	4.7	3.52	64.18	1.93	2.53	0.32	0.65	1.2	1.2	6.5	57.85	3.15	3600
Ns	23.6	0.13	0.07	0.07	0.05	0.1	9.3	0.12	–	–	–	–	1.2	–
Ms	89.6	–	–	–	–	–	0.11	0.3	3.8	–	–	–	1.9	220,000

Table 2
Mix design.

NO.	C (gr)	W/C	S/C	Ns/C	Ms/C	W/B
1	1200	0.500	2.667	0.000	0.000	0.50
2	1152	0.521	2.778	0.000	0.042	0.50
3	1092	0.549	2.930	0.000	0.099	0.50
4	1044	0.575	3.065	0.000	0.149	0.50
5	1183.2	0.507	2.705	0.014	0.000	0.50
6	1166.4	0.514	2.743	0.029	0.000	0.50
7	1149.3	0.522	2.784	0.044	0.000	0.50
8	1135.2	0.529	2.819	0.015	0.042	0.50
9	1118.4	0.536	2.861	0.030	0.043	0.50
10	1101.3	0.545	2.906	0.046	0.044	0.50
11	1075.2	0.558	2.976	0.016	0.100	0.50
12	1058.4	0.567	3.023	0.032	0.102	0.50
13	1041.3	0.576	3.073	0.049	0.104	0.50
14	1027.2	0.584	3.115	0.016	0.152	0.50
15	1010.4	0.594	3.167	0.033	0.154	0.50
16	993.3	0.604	3.222	0.051	0.157	0.50
17	1200	0.400	2.667	0.000	0.000	0.40
18	1152	0.417	2.778	0.000	0.042	0.40
19	1092	0.440	2.930	0.000	0.099	0.40
20	1044	0.460	3.065	0.000	0.149	0.40
21	1183.2	0.406	2.705	0.014	0.000	0.40
22	1166.4	0.412	2.743	0.029	0.000	0.40
23	1149.3	0.418	2.784	0.044	0.000	0.40
24	1135.2	0.423	2.819	0.015	0.042	0.40
25	1118.4	0.429	2.861	0.030	0.043	0.40
26	1101.3	0.436	2.906	0.046	0.044	0.40
27	1075.2	0.446	2.976	0.016	0.100	0.40
28	1058.4	0.454	3.023	0.032	0.102	0.40
29	1041.3	0.461	3.073	0.049	0.104	0.40
30	1027.2	0.467	3.115	0.016	0.152	0.40
31	1010.4	0.475	3.167	0.033	0.154	0.40
32	993.3	0.483	3.222	0.051	0.157	0.40

C = Cement, W/C = Water to Cement ratio, S/C = Sand to Cement ratio, Ns/C = Nano silica to Cement ratio, Ms/C = Micro silica to Cement ratio and W/B = Water to Binder ratio.

the immersed specimens underwater (W_w) and also the saturated surface dry condition (W_{ssd}) were measured. The calculated porosity value using following equation:

$$P = \frac{W_{ssd} - W_d}{W_{ssd} - W_w} \times 100 \quad (1)$$

2.3. FE-SEM image

In order to specify the effect of porosity values on the microstructure in different phases of cement mortar, the Field Emission Scanning Electron Microscope (FE-SEM) image was applied on specimens (with a volume of less than 1 cm^3). For this purpose, the small pieces were taken from virgin cement mortar specimens which were cured for 28 days and then soaked in ethanol for over a week to stop the chemical reactions. The image scanning was done by (Hitachi-S-4160, Japan) apparatus in 1000× magnification and 20 kV voltage.

3. Experimental results

3.1. Porosity

Figs. 1 and 2 show the results of porosity for 32 mix designs which are containing various percentages of Ns and Ms at different ages (3, 7, 14, 21, and 28 days) with W/B ratio of 0.50 and 0.40, respectively. It is worth noting that the porosity values have been measured by the Archimedes' principle (Eq. (1)) .Fig. 1a shows that the porosity of control mortar (0% Ms + 0% Ns) is by 20% at the age of 3 days, and it decreases to 15% while the Ns is increased up to 4.2%. It can be observed from Fig. 1a that simultaneous increase of Ns and Ms in mix designs led to a reduction in porosity compared to the mixture merely containing Ns. For instance, the porosity of mixtures which are containing by 4% Ms + 2.8% Ns and 9% Ms + 2.8% Ns are lower than the mixture containing by 2.8% Ns. Fig. 1a shows that the lowest porosity is by 13.5% in mixture of 9% Ms + 2.8% Ns. It can be indicated by increasing the age of specimens from 3 to 28 days, along curing time of specimens, the hydration process is complete with the water existence in specimens. Moreover, the space which is belonging to water and pores with formation calcium silicate hydrate (C—S—H) and calcium hydroxide (CH) led to a reduction in the porosity. In fact, it is confirmed by other studies that increasing specimen's age containing Ns and Ms would form a denser structure due to hydration process between cement and pozzolanic materials [33]. It is noted in Fig. 1e that the 28-day porosity values have decreased significantly compared to the respective early age values. For example, the 28-day porosity with 4% Ms + 4.2% Ns is by 8.5%, while the porosity amounts of 14 and 3 days for respective mixture are by 12% and 16.5%, respectively. Among all mixtures, the lowest value of 28-day porosity for 9% Ms + 2.8% Ns is by 7%. The current study results have confirmed the findings of previous studies [34-36].

According to Fig. 2a, for W/B ratio 0.40 the porosity of the control mortar (0% Ms + 0% Ns) is altered from 16% to 12% when Ns increases up to 4.2%. As similar to Fig. 1a, the porosity value of mixture containing by 4% Ms + 1.4% Ns and by 9% Ms + 1.4% Ns is lower than the mixture with merely 1.4% Ns as shown in Fig. 2a. With the change of W/B ratio from 0.50 to 0.40 and, following that, the reduction of water value, the denser structure has appeared with the better formation of hydration products and it has led to prevent the porous structure; consequently, the porosity values got reduced [36]. Also, Qian et al. [37] reported that the presence of the replacement cementitious material in cement mixtures has decreased the proportion of unhydrated cement in mixtures, so that, a larger volume of C-S-H gel make much more compact's cement mortar matrix. Nevertheless, the porosity trend of the mixtures with W/B of 0.50 is the same as W/B of 0.40, but the porosity values for W/B of 0.40 are significantly lower than W/B of 0.50.

3.2. Compressive strength

Relations of F_c with four different percentages of Ms (0%, 4%, 9% and 13%) and Ns (0%, 1.42%, 2.8% and 4.2%), considering ages of specimens (3, 7, 14, 21, and 28 days), are shown in Figs. 3 and 4 while the W/B ratios are 0.50 and 0.40, respectively. Figs. 3 and 4 show that the lowest compressive strength has appeared in the control mortar (0% Ms + 0% Ns); it doesn't have any pozzolanic materials, so it has the highest values of porosity. Fig. 3 shows that the compressive strength of control mortar with W/B of 0.50 is altered from 18 MPa to 50 MPa while this increased strength, due to a reduction in porosity value, has been observed in Fig. 1 from 20% to 9%. In a similar trend, Figs. 2 and 4 show that the changes of compressive strength and porosity for W/B of 0.40 are from 25 MPa to 57 MPa and from 16% to 6.5%, respectively. It is clear that decreasing mortar porosity, increasing the age of specimens and completing the hydration process led to an increase in compressive strength [38]. Increasing Ns in the mixtures which are containing merely Ns causes an increase in compressive strength as shown in Figs. 3 and 4. For instance, in W/B of 0.50 and 0.40, the 3-day compressive strength was respectively altered from 18 MPa to 33 MPa and from 25 MPa to 37.2 MPa, while the Ns was altered from 0% to 4.2%. The effect of the simultaneous increase in Ms and Ns is higher on the early age specimens. For example, the highest 3 and 28 day compressive strength (9% Ms + 2.8% Ns), compared to respective control mortar (0% Ms + 0% Ns), for W/B of 0.50, was growing up approximately about 145% and 54%, respectively, while the porosity reduction values were

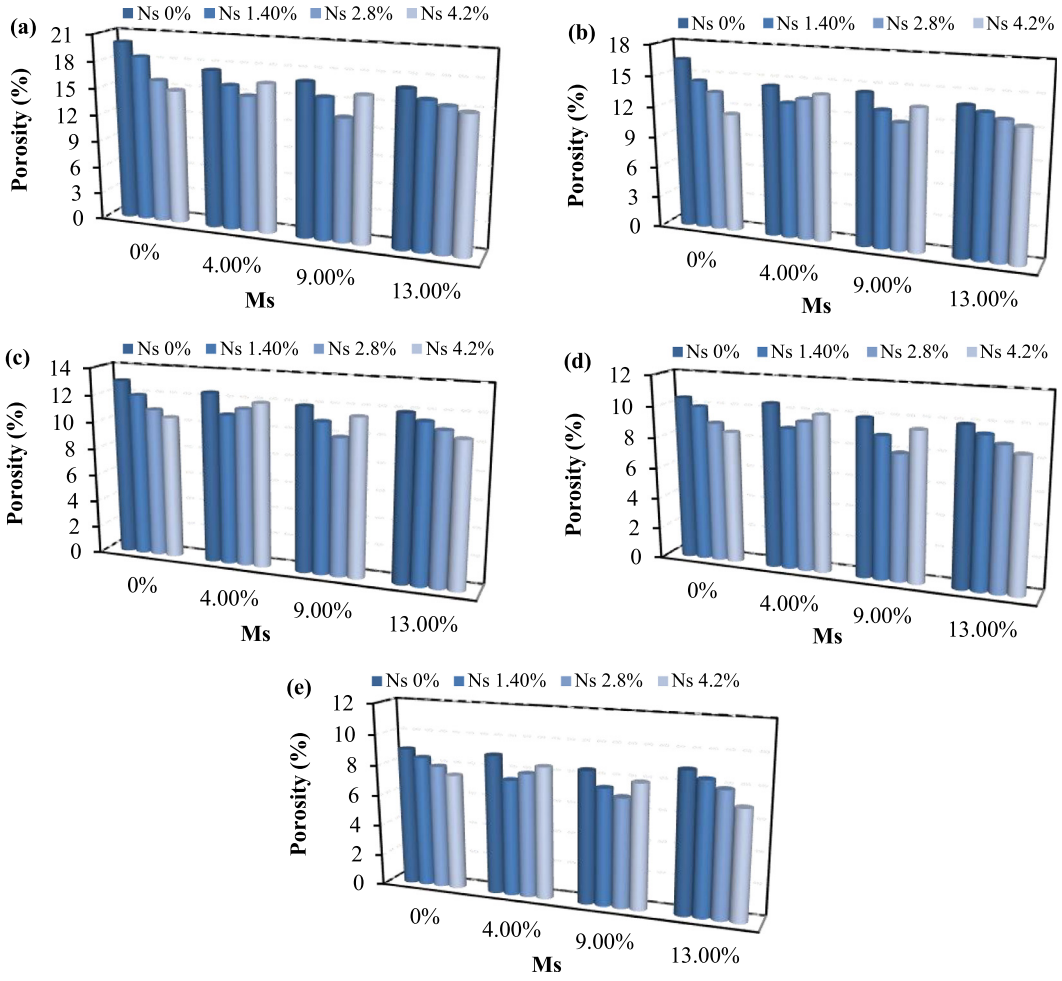

Fig. 1. Relation of porosity with Ms% and Ns% in W/B of 0.50 for different ages: (a) 3, (b) 7, (c) 14, (d) 21 and (e) 28 days.

by 32.5% and 22.2%, respectively. In this regard, Jalal et al. [39] investigated the effect of Ns and Ms on cement-based materials. Their results indicated that the simultaneous presence of Ns and Ms has the better effect on cementitious materials. The current results show that the simultaneous increase in Ms and Ns has improved compressive strength, while the highest compressive strength of 28 days for W/B of 0.50 and 0.40 had appeared in 9% Ms + 2.8% Ns. Moreover, the compressive strength of mortar is a function of W/B ratio that affects the porosity values so that the lower W/B ratio is the larger compressive strength [20].

3.3. Flexural strength

Fig. 5a and b show the flexural strengths of cement mortar specimens containing various percentages of Ns and Ms at the age of 28 days while the W/B ratios were equal to 0.50 and 0.40, respectively. Fig. 5 shows that flexural strength of the control mortar (0% Ms + 0% Ns) is the lowest amount because it approximately has the highest porosity in comparison to the other mixtures. The flexural strength of mixtures which was merely containing Ns for W/B ratios of 0.50 and 0.40 was altered from 7.5 to 10.8 and 8.6 to 12.2, respectively, and also the porosity values were altered from 9% to 7.5% and 6.5% to 5%, respectively. The simultaneous increase of Ms and Ns increases the flexural strength of the mixture with merely Ns, while higher flexural strength has appeared in the lowest W/B ratio and porosity [20]. For instance, the flexural strengths of mixtures containing by 9% Ms + 1.4% Ns and 13% MS + 1.4% Ns for W/B of 0.50 are 10.5 MPa and 10.2 MPa, respectively, while these values for W/B of 0.40 are 12 MPa and 11.5 MPa, respectively. The highest flexural strengths for W/B of 0.5 and 0.40 were 11.6 MPa and 12.8 MPa in mixture of 9% Ms + 2.8% Ns. In fact, the porosity value in W/B of 0.40 is lower than W/B of 0.50, thus the maximum flexural strength has appeared in the W/B ratio of 0.40. From Fig. 5 it is generally concluded that the simultaneous increase of Ms and Ns reduces the porosity values, and the flexural strength has been improved ultimately.

3.4. FE-SEM analysis

The FE-SEM images of cement mortar specimens which are containing by 0% Ms + 0% Ns, 13% Ms + 0% Ns, 0% Ms + 4.2% Ns, and 9% Ms + 2.8% Ns with W/B of 0.50, and 0.40 are shown in Figs. 6 and 7, respectively. It can be seen from Figs. 6a and 7a that the control mortar (0% Ms + 0% Ns) has an approximately loose microstructure due to fairly huge crystals and voids. Still some huge crystal is formed in the mixture with the only presence of Ms or Ns, but the fewer voids and smaller crystal size led to the formation of the more compact microstructure, as shown in Figs. 6b-c and 7b-c. This fact by Qing Y et al. [40] is pointed out that the Ms plays two roles in cement mortar microstructure, (1) a chemical inert filler and (2) pozzolanic reaction. Their results have shown that the chemical inert filler properties led to improve the physical structure and provide nucleation sites for hydration products while the pozzolanic reaction leds to chemical act with CH gel that

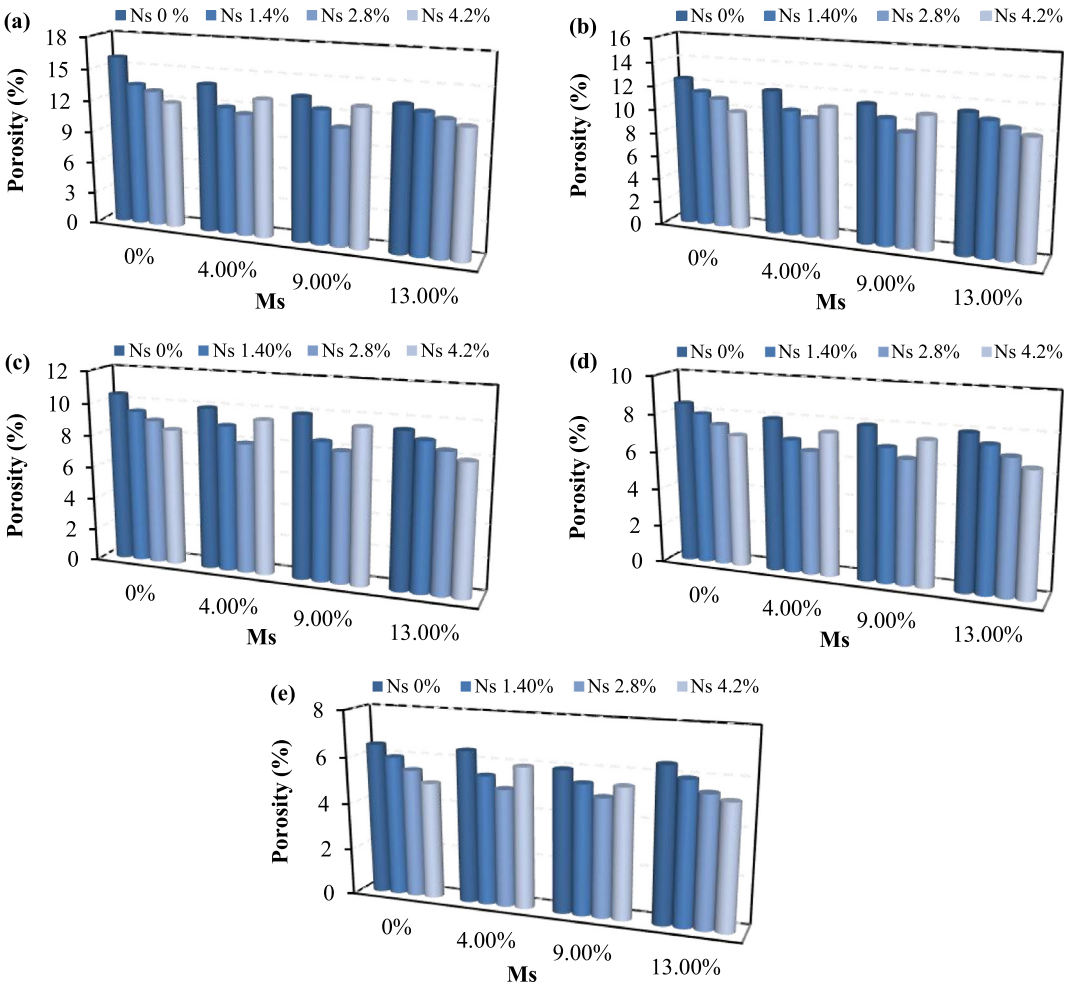

Fig. 2. Relation of porosity with Ms% and Ns% in W/B of 0.40 for different ages: (a) 3, (b) 7, (c) 14, (d) 21 and (e) 28 days.

appeared during hydration of cement and eventually improved the paste-aggregate bond. The silica pozzolanic reaction between Ns and calcium hydroxide led to developed more C—S—H gel and decreased the calcium leaching rate of cement mortar, which is in agreement with previous studies [40,41]. This is due to the fact that Ns is approximately 100 times smaller than cement particles, so it is able to fill remaining voids and eventually form more uniform and dense microstructure [42]. As shown in Figs. 6b-c and 7b-c, the Ns has the better modification effect compared to Ms due to its larger surface area, so a smaller value of nano silica additive in mixtures such as 0%Ms + 4.2%Ns has more effective influence against the mixtures containing higher values of Ms. Moreover, Figs. 6d and 7d indicated that the presence of both Ms and Ns exhibits much fewer huge crystals, and also the dense compact texture has appeared. It is vindicable that the overlapping effect of nano silica and micro silica on the filling of voids so that Ms particles would have filling role between cement particles, also the Ns particles would play this role between the cement particles and Ms. In this way, the best utilization of Ms and Ns is due to the best performance of Ms on filling voids and high reactivity pozzolanic performances of Ns. This is while other studies have pointed out the synergistic presence of Ms and Ns would allow the further increase strength, sulfate resistance, and carbonation resistance than that adding Ms or Ns alone [21]. These observations reveal the synergetic effect of Ms and Ns which leads to densify the microstructure, fill the pore structures, and induce the higher forms of C—S—H gel due to the dense structure [20].

4. Artificial neural networks methods

Artificial Neural Network (ANN) is a mathematical or computational model which is similar to human brain that uses an interconnected series of neurons for information processing based on a connectionist approach to prediction. Moreover, ANN model is able to learn highly complex and nonlinear data in an instant, the data which is usable in our approach with experimental and statistical data. The fundamental strategy for the development of ANN model is trying to make progress on experimental output data in material behavior. If the experimental results include information which is related to material behavior, training ANN with sufficient information of materials behavior could provide a qualified model [43]. Network training with more samples increases the number of iteration and leads to prevention of early convergence and hits lower error [44]. A general ANN model consists of three main layers: input, hidden, and output layers. In the input and output layers, the number of neurons is equal to the number of input and output parameters, while the number of neurons in the hidden layer depends on the type of problem.

4.1. Data preparation of ANN

A model feed-forward neural network is used in this study. The activation functions are nonlinear for neurons' hidden layer and the neuron outputs. The fundamental principle of the developing

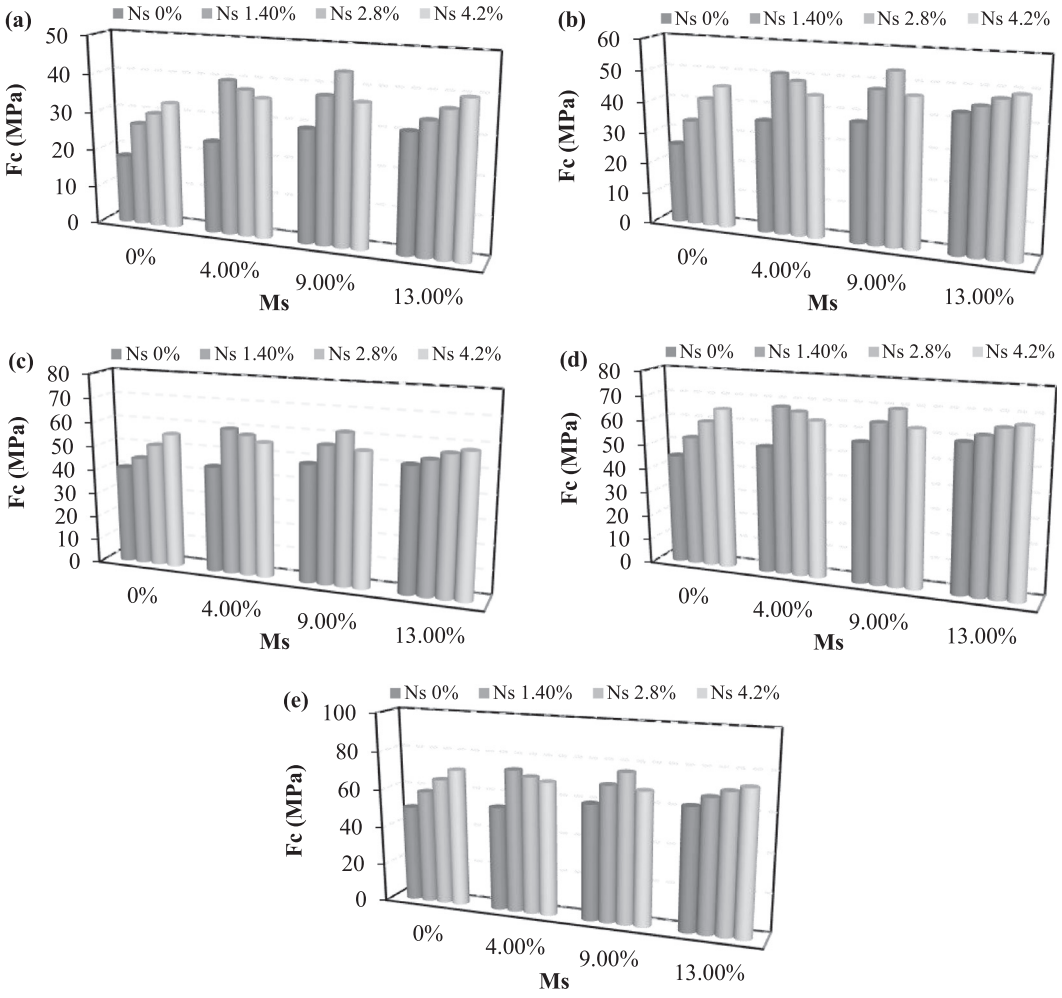

Fig. 3. Relation of Fc with Ms% and Ns% in W/B of 0.50 at different ages: (a) 3, (b) 7, (c) 14, (d) 21 and (e) 28 days.

neural network in this research has been carried out on two models by Alyuda NeuroIntelligence tools [45]: (1) ANN-I model is without considering porosity as input parameter and (2) ANN-II model is with considering porosity as an input parameter. Therefore, the ANN-I model consists of one input node less than the ANN-II. Since in composite materials like cement mortar, the result accuracy of the ANN model depends on data quality, in order to do an accurate and qualified prediction, the effective variable ratios between materials such as W/C, S/C, Ns/C, Ms/C are expressed, not the individual variables such as water, sand, nano silica, micro silica, and etc. The hyperbolic tangent (tanh) functions are adopted for both input and output functions after normalizing the original data, while the applied output learning rate and iteration number were equal to 0.1 and 1000, respectively [46].

The input parameters in compressive and flexural strength method, considering the porosity are 7 and 6 and without considering the porosity are 6 and 5, respectively (specimen's age in the flexural method is 28 days). Therefore, considering these input nodes and one hidden layer, the target node is the compressive and flexural strengths of specimens, respectively. The used neural network architecture in this study was called ANN N_i-N_h-1, where N_i and N_h are the numbers of input and hidden layer nodes, respectively, and the third part is described as the number of output as shown in Table 3. The architecture of ANN models for prediction of compressive and flexural strengths, is illustrated in Fig. 8 with or without considering porosity.

4.2. Error estimation

In order to evaluate the ANN model performance, these are used: criteria for selecting of minimum errors of MAPE, RMSE and best adaptation of ANN predicted results with actual results on the basis of the coefficient of determination (R^2). If we assume that the actual and predicted values for ith data from the total number of data (n) are respectively A_i and P_i , then, Mean Absolute Percentage Error (MAPE) and Root Mean Square Error (RMSE) have been used to evaluate the accuracy of the ANN model according to Eqs. (2) and (3), respectively.

$$\mathrm{MAPE} = \frac{1}{n}\sum_{i=1}^{n}\left|\frac{A_i - P_i}{A_i} \times 100\right| \tag{2}$$

$$\mathrm{RMSE} = \sqrt{\frac{1}{n}\sum_{i=1}^{n}(A_i - P_i)^2} \tag{3}$$

5. Genetic algorithm programing

John Holland [47] showed how an evolutionary process can be used to solve various problems. These problems are solved using a strongly-parallel technique that is now called the Genetic Algorithm (GA). GA is a string of numbers which has been made in

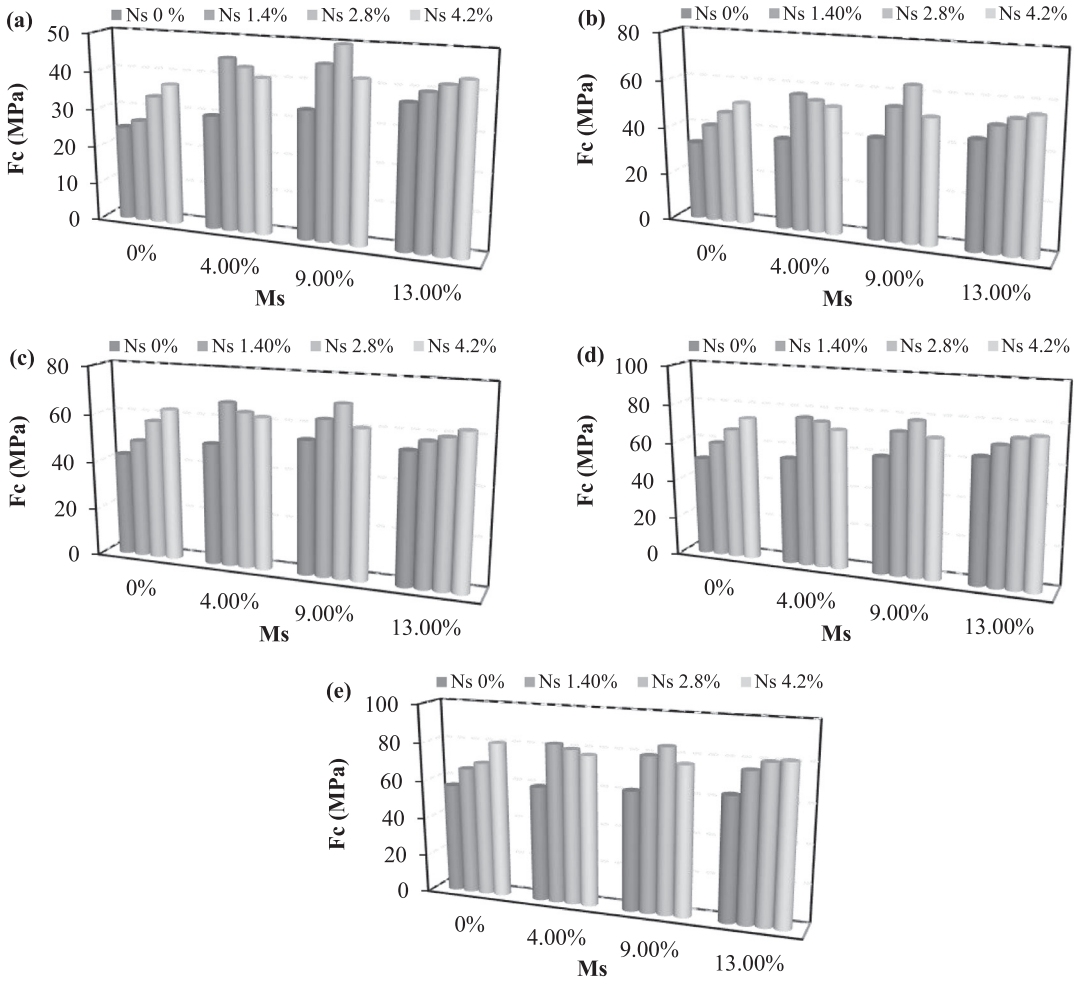

Fig. 4. Relation of Fc with Ms% and Ns% in W/B of 0.40 at different ages: (a) 3, (b) 7, (c) 14, (d) 21 and (e) 28 days.

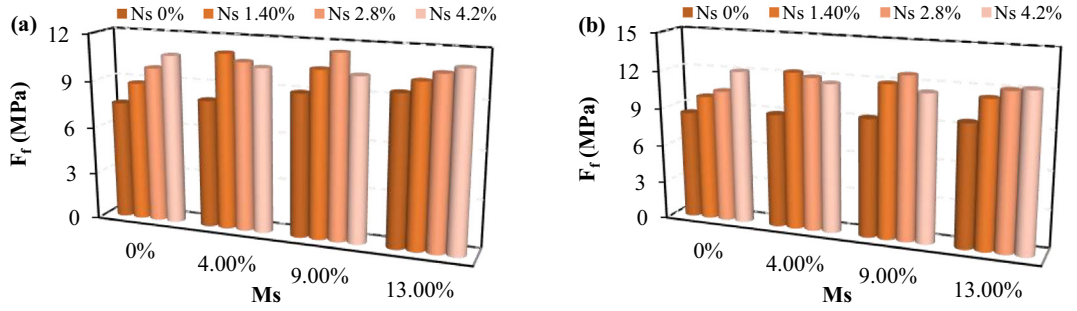

Fig. 5. Relation of Ff with Ms% and Ns% at age of 28 days in W/B of (a) 0.50 and (b) 0.40.

order to develop Genetic Program (GP) that was proposed by Koza in 1992 [48]. In fact, GP is an evolutionary algorithm that inspired Darwin's theory which set people with a different feature to a new collection of individuals who have different and specific features. The early pioneers in GP found that it is able to solve or approximately solve problems which are based on Darwin's principle of reproduction and analogs of naturally-occurring genetic operations such as selection, mutation, and crossover [49]. GPs are a computer programs to solve problems which have been expressed in a functional programming language and embodied as tree structures [50]. Fig. 9 shows the GP flowchart solve problems. There are three steps in GP as the following:

(1) Set an initial population of individuals with fixed-length strings randomly. In fact, there has been initial population for the parents from the first generation.
(2) Repeat the following steps to create termination criteria.
(2-1) Population fitness must be measured, then fitness value will be assigned to individuals. In fact, F_c and F_f of cement mortars are assigned to the individuals as fitness valuable.

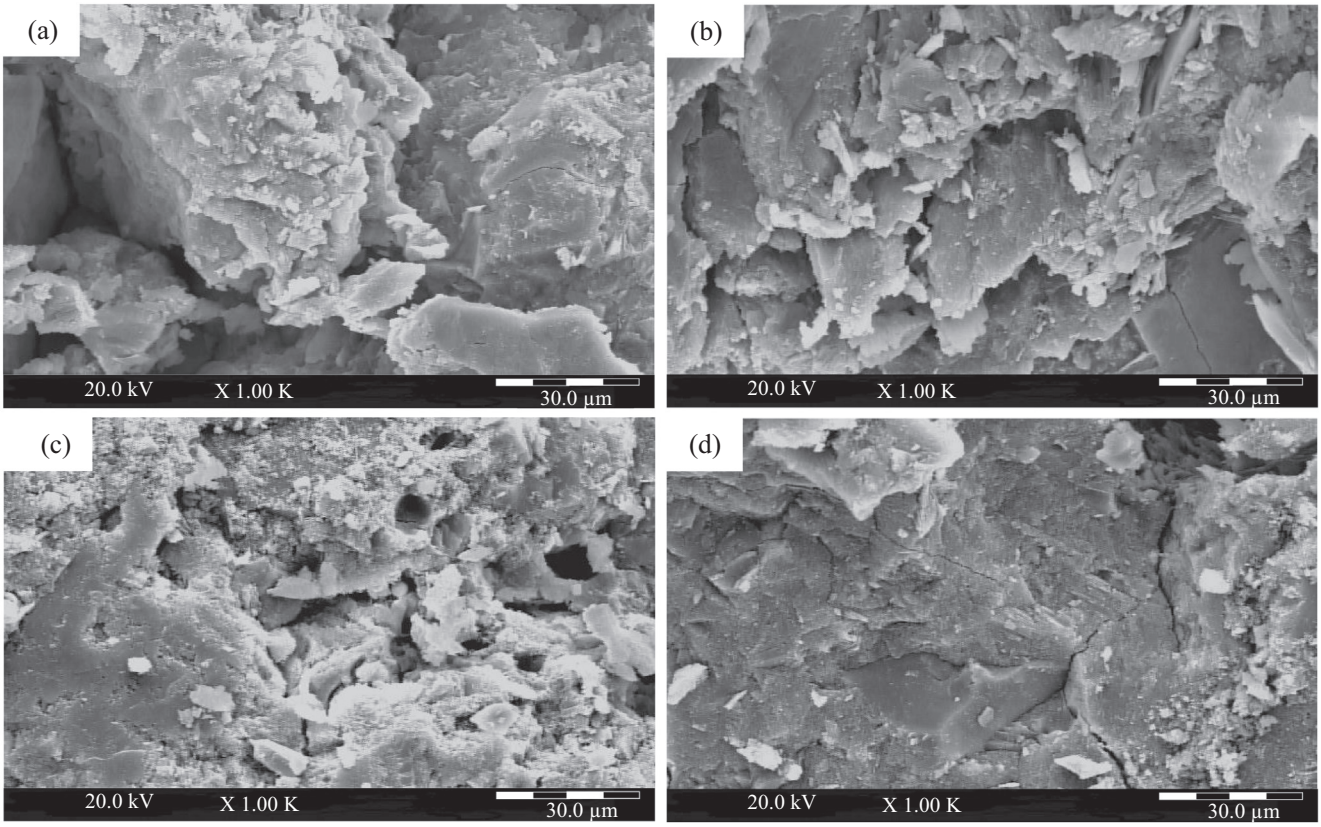

Fig. 6. SEM image of mortar with W/B of 0.50: (a) 0%Ms + 0%Ns, (b) 13%Ms + 0%Ns, (c) 0%Ms + 4.2%Ns (d) 9Ms + 2.8%Ns.

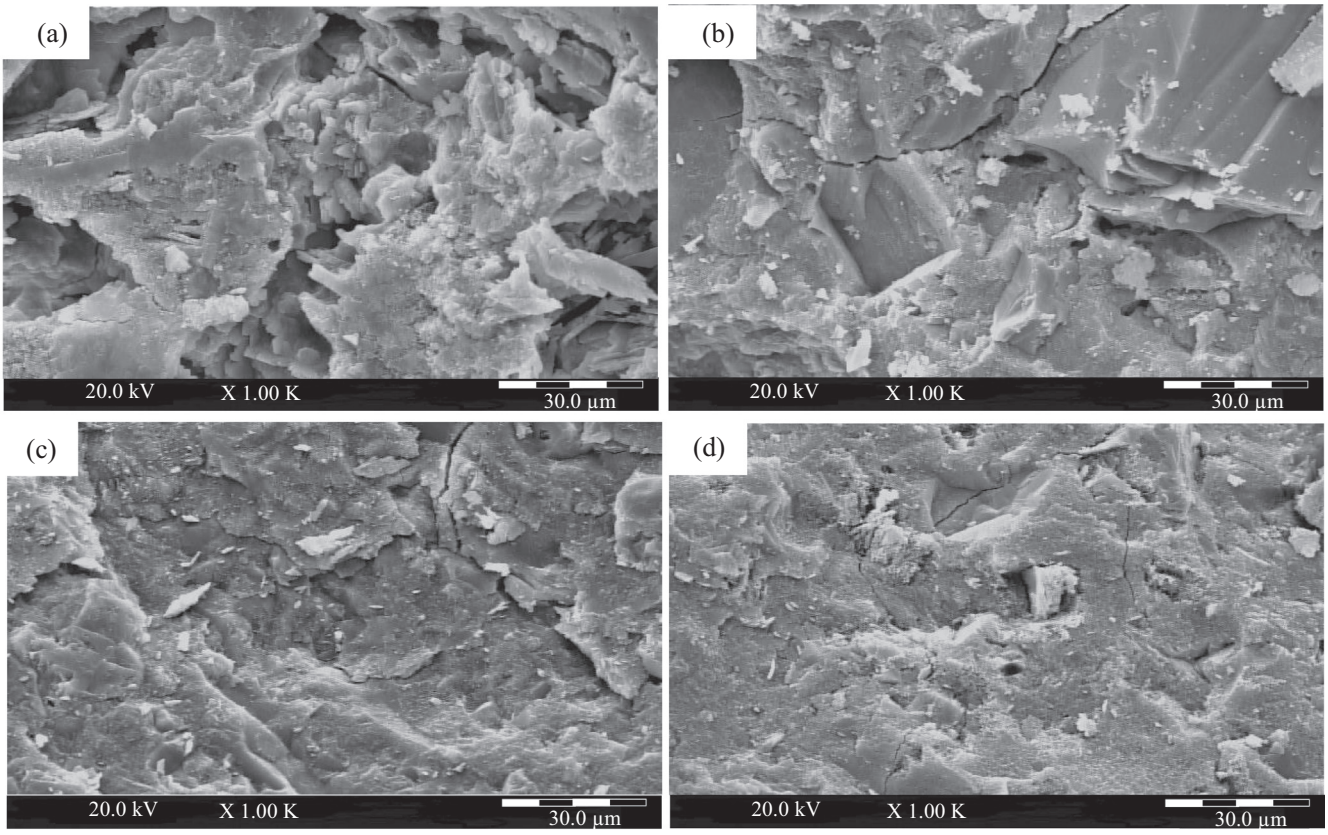

Fig. 7. SEM image of mortar with W/B of 0.40: (a) 0%Ms + 0%Ns, (b) 13%Ms + 0%Ns, (c) 0%Ms + 4.2%Ns (d) 9Ms + 2.8%Ns.

Table 3
Neural network parameters.

Parameter	ANN model			
	ANN_{Fc}-I	ANN_{Fc}-II	ANN_{Ff}-I	ANN_{Ff}-II
number of specimens	480		96	
number of input layer neurons (N_i)	6	7	5	6
number of hidden layer neurons ($N_{h)}$	1		1	
number of output layer neurons	1		1	
number of iteration	1000		1000	
activation function	hyperbolic tangent		hyperbolic tangent	

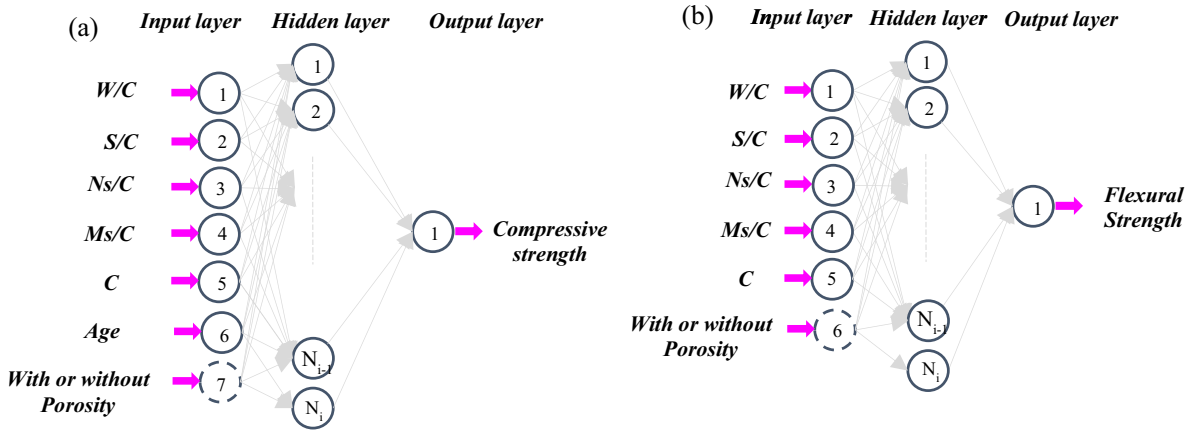

Fig. 8. ANN architecture for prediction of compressive and flexural strength: (a) ANNFc and (b) ANNFf.

(2-2) A new population of strings is made with the following three genetic steps.
(i) Existing individual strings are copied up to cause the reproduction of population.
(ii) Crossover operation at the crossover point randomly formed the two new strings from the two existing strings by genetic operation.
(iii) Random mutations can build the new string from previous string while the position in the string is chosen randomly.
(3) The string that is analyzed as a result by genetic method is run that might be a solution to the problem.

The GA and GP are similar to each other in many aspects; however, the individual representation clearly shows the distinctions between them. In fact, the individuals in the GA and GP are strings of binary digits with fixed lengths and derives parse trees with different size and shapes, respectively.

5.1. Theory of genetic expression programs

In the following extension of GA and GP, Genetic Expression Program (GEP) was introduced by Ferreira [51]. GEP is the computer program based on an evolutionary algorithm. The GEP, due to having linear and nonlinear chromosomes, is alike GA and GP, respectively [51]. Individual GEP is similar to GP in that they are both considered as represented trees (expression trees), but contrary to GP, there are empty spaces (tails) in GEP for each gene after encoded parts (head). The encoded chromosomes which have branch structures are named Expression Trees (ETs). In ETs, the head of gene is decoded; the program is converted the linear input to nonlinear output by the used element that fills the tails. Eventually, the linking of genes is accomplished using linking functions to the formation of chromosomes [52]. Due to empty space and the genetic reliance on lisp, Karva language is considered as one of the GEP benefits. The above-mentioned content is shown in Fig. 10 [53]. Generally, the task of algorithm processing and operation in GEP is similar to GA and GP.

5.2. Genetic expression programming structure and parameters

In this study, to evaluate the effect of porosity and various percentages of nano and micro silica in cement mortar's strength, the GEP modeling has been applied by software GeneXpro Tools 5.0 [54]. It's noted that the GEP modeling has been done in two approach addition and multiplication, while compressive and flexural strengths were considered as output parameters. The input parameters in GEP modeling were W/C and S/C ratios, Ns/C and Ms/C ratios, cement weight, age of specimens, and porosity. The fundamental principle of the developed GEP model in this research has been carried out on two model: (1) GEP-I model is without considering porosity as an input parameter and (2) GEP-II model is with considering porosity as an input parameter. The details of GEP-I and GEP-II models are presented in Table 4 for addition and multiplication approach.

In each compressive and flexural model, 130 and 26 data numbers are respectively used for training, and 30 and 6 data numbers are respectively used for testing.

While the model is generated to achieve minimum error, the individual converge with the best fitness has appeared on chromosomes. There is a mathematical relationship between the final chromosomes of the expression tree, which specifies the relation between input and output variables. The training and testing parameters which have been used in GEP-I and GEP-II models, both addition and multiplication approaches, were mentioned in Table 5.

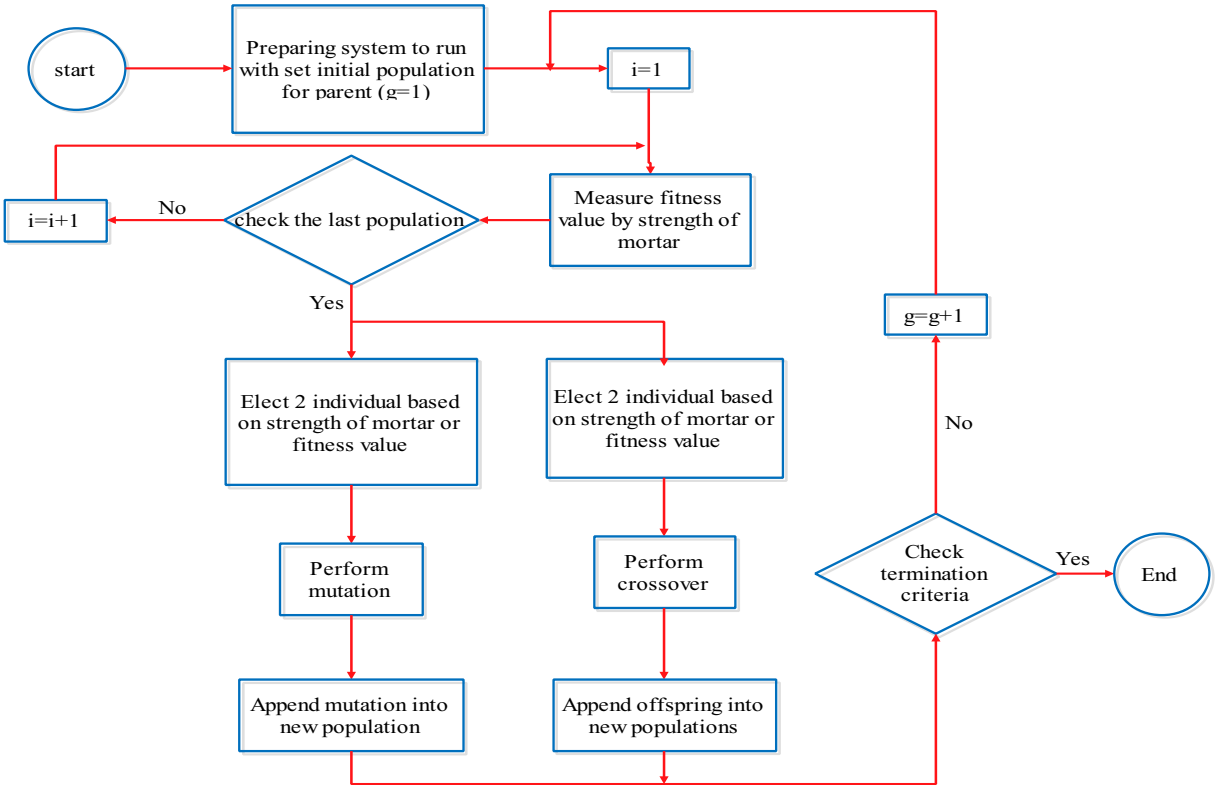

Fig. 9. Genetic programing flowchart.

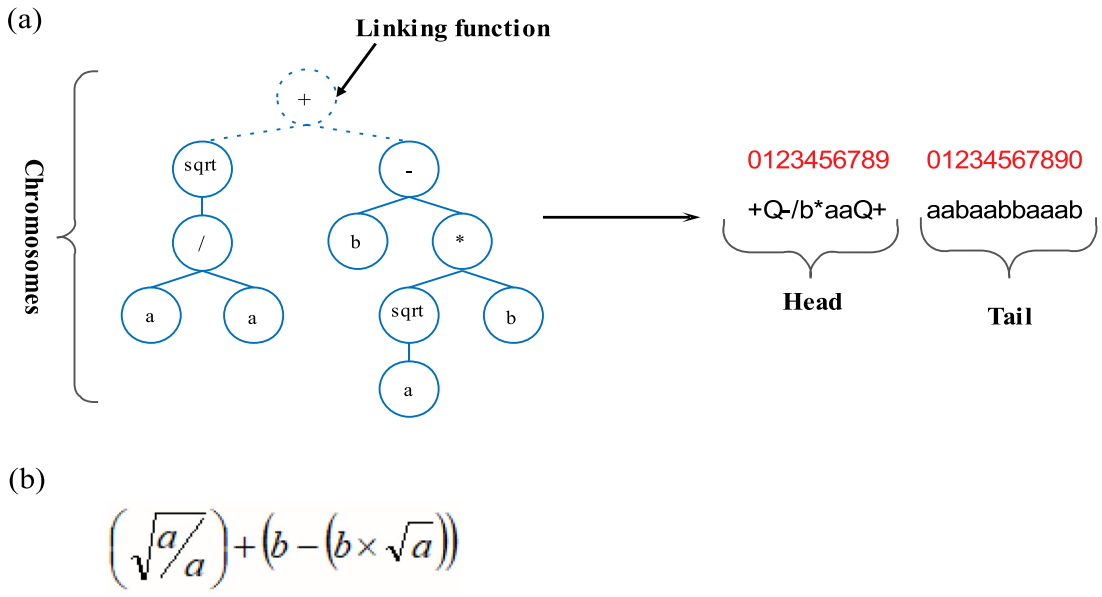

Fig. 10. Chromosomes representation tree in LISP (a), mathematical formulation (b) [51].

6. Modeling results

6.1. ANN models

Figs. 11 and 12 show the comparison between experimental and ANN predicted results in the form of ANN-I and ANN-II models. Fig. 11 indicates that ANN-I model has significant dispersion between experimental and predicted results, due to ignoring porosity as an input values. The performance of ANN-I model for compressive and flexural strength results show that ANN-I model predicts the compressive and flexural strengths of cement mortar without considering porosity, while the pair of compressive and flexural training R^2 and compressive and flexural testing R^2 values were (0.9301, 09232) and (0.8961, 0.8699), respectively.

The ANN-I model indicated that the dispersion of data and the error values were almost high between experimental and predicted data due to neglecting the porosity in the model performance as shown in Fig. 11. For better perception, one must note

Table 4
GEP input parameters.

Model GEP				
Approach	Addition and Multiplication			
Model	GEP_{Fc}-I	GEP_{Ff}-I	GEP_{Fc}-II	GEP_{Ff}-II
Input parameters	W/C, S/C, Ns/C, Ms/C, C, Age	W/C, S/C, Ns/C, Ms/C, C	W/C, S/C, Ns/C, Ms/C, C, Age, P	W/C, S/C, Ns/C, Ms/C, C, P

Table 5
Parameters of GEP models.

Parameter	Definition	GEP-I / GEP-II
P1	Function set	+, −, *, /, sqrt, Exp, Ln, 3Rt, sin, cos, Arc tan, x^2, x^3
P2	chromosomes	30
P3	Head size	10
P4	Number of gene	4
P5	Linking function	Addition and Multiplication
P6	Mutation rate	0.002
P7	Inversion rate	0.005
P8	One-point recombination rate	0.003
P9	Two-point recombination rate	0.003
P10	Gene recombination rate	0.003
P11	Gene transposition rate	0.003
P12	Constant per gene	10

the fact that each cement mixture has a different porosity, and it's clear that the porosity affects both compressive and flexural strengths, so neglecting to consider porosity as an input parameter causes a significant error. Therefore, in order to evaluate the sensitivity of porosity in the model performance, the ANN-II model was proposed, while the porosity values were considered as the input parameter.

Fig. 12 shows the ANN-II model of the experimental and predicted strengths of cement mortar. The models with the low RMSE and MAPE and high R^2 values are able to predict the compressive and flexural strengths with high accuracy. From the figure it can be seen that there was close dispersion data and so less error in the ANN-II model, while the pair of compressive and flexural training R^2 and compressive and flexural testing R^2 values were (0.9965, 09843) and (0.9467, 0.9702), respectively.

The statistical values of the training and testing sets of the ANN-I and ANN-II for both compressive and flexural strengths are presented in Table 6. The closest values of R^2 to 1 and the less value of error (MAPE and RMSE) are the best ANN model, so the ANN-II was the best proposed model while the triplet value of compressive training R^2, MAPE, and RMSE were equal to 0.9965, 1.415, and 0.862, respectively, and the flexural testing values were equal to 0.9883, 0.914, and 0.801, respectively.

6.2. GEP models

6.2.1. Addition and multiplication models of GEP_{Fc}-I and GEP_{Ff}-I

The mathematical non-linear formulations for predicted relations between mechanical properties and input variables from trees (GEP_{Fc}-I and GEP_{Ff}-I) were shown in Eqs. 4–7 while they have been considered both addition and multiplication approach. For instants, the ETs of the formulation in the Eq. (4) is shown in Fig. 13 for the GEP_{Fc}-I.

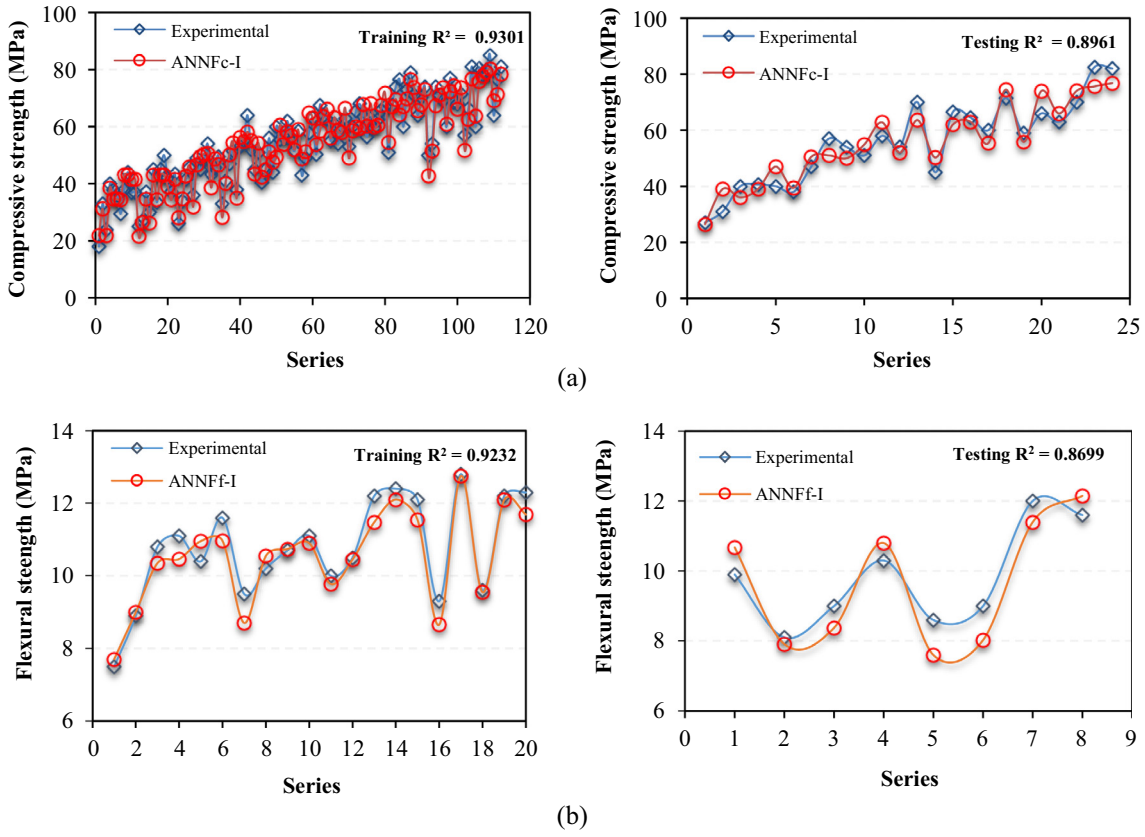

Fig. 11. Evalution of experimental and predicted results: (a) compressive strength and (b) flexural strength by ANN-I models.

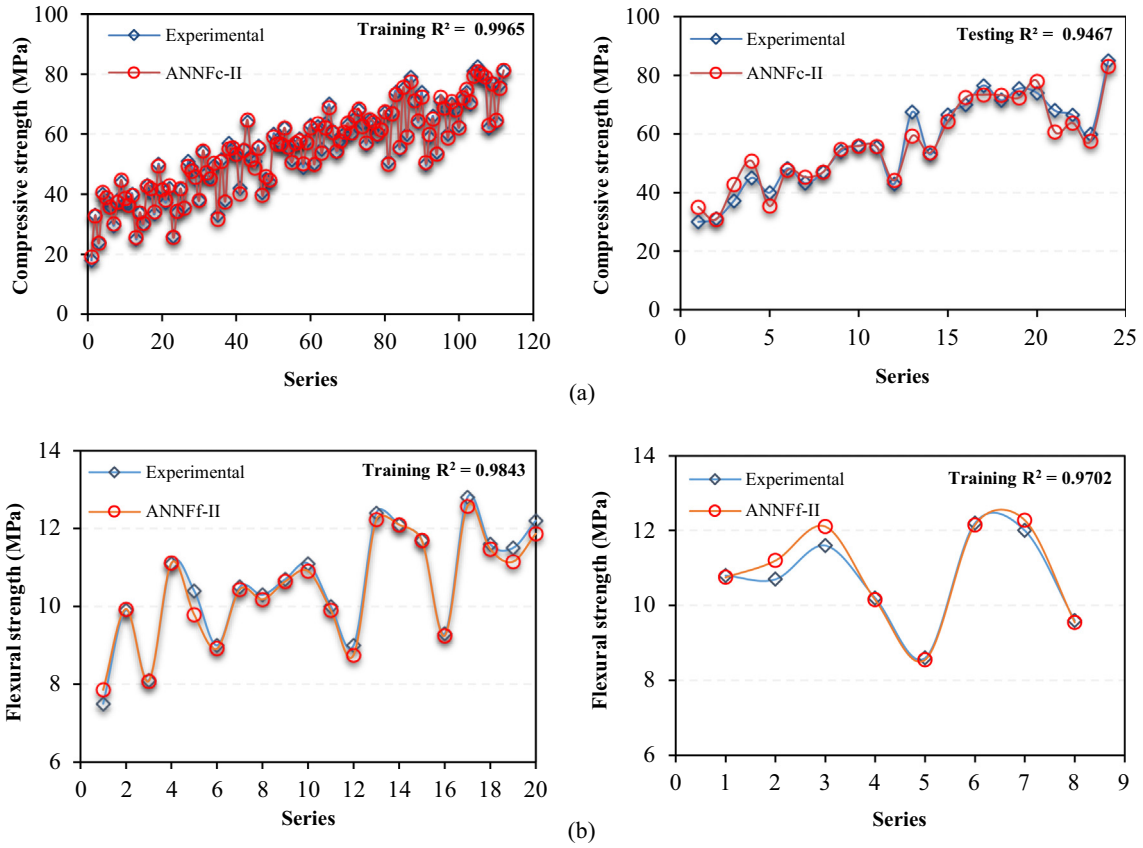

Fig. 12. Evalution of experimental and predicted results: (a) compressive strength and (b) flexural strength by ANN-II models.

Table 6
Statistical values of ANN-I and ANN-II models.

Model	Condition	R^2		MAPE		RMSE	
		Training	Testing	Training	Testing	Training	Testing
ANN-I	Compressive strength	0.9301	0.8961	6.372	8.025	3.946	4.725
	Flexural strength	0.9232	0.8699	3.390	6.766	0.444	0.697
ANN-II	Compressive strength	0.9965	0.9467	1.451	5.182	0.862	3.558
	Flexural strength	0.9843	0.9702	1.537	1.725	0.221	0.272

$$GEP_{Fc}-I=(C)^{0.25}\times\mathrm{Cos}\left(\mathrm{Ln}\left[\left(\frac{W}{C}\right)^{3}\times\mathrm{Cos}\left(\sqrt[3]{\frac{S}{C}}\right)\right]\right)+\left[(Ns)^{0.25}\times\frac{93.935C}{S}\right]^{0.5}+\mathrm{Age}+\left[(\mathrm{Arc\,tan\,C})\times\mathrm{Arc\,tan}\left(-9813.979\times\mathrm{Cos}\left(\frac{S}{C}\right)^{2}\right)\right]-14.614+\left[\mathrm{Arc\,tan}(\mathrm{Age})\times\mathrm{Ln}\left(\frac{S}{C}\right)\times C^{0.5}\right] \quad (4)$$

$$GEP_{Ff}-I=\mathrm{Sin}\left[\left(\frac{(41.276)^{2}}{-41.276+\frac{S}{C}}\right)+\left(38.458\times\frac{Ns}{C}\right)\right)+\left(\frac{S}{W}\times\mathrm{Cos}\frac{Ms}{C}\right)\Bigg]+\left[\mathrm{A\,tan}\left(\mathrm{Cos}^{3}C\times\sqrt[3]{\frac{Ns}{C}}\times(-13.998)^{2}\right)\right]^{2/3}+\left[\mathrm{Cos}\left(\left(e^{-3.720}+\frac{S}{C}\right)-\left(\frac{Ns}{C}+\frac{S}{C}\right)^{2}\right)+\sqrt[3]{\frac{Ms}{C}}\right]+\mathrm{Ln}\left[\left((Ms)^{1/3}+78.930\right)+\left(e^{-8.572}\right)^{1/3}\right]^{2} \quad (5)$$

$$GEP_{Fc}-I=e^{\left[\left(\frac{Ns}{C}\right)+\sin\left(\mathrm{Ln}\left(\frac{W}{C}+\mathrm{Age}\right)^{1/3}\right)^{1/3}\right]}\times\left[\left((-67.253)^{2}\times81.905\times\frac{Ns}{C}\right)^{1/27}+\frac{S}{C}\right]^{0.5}\times\mathrm{Ln}\left[C-e^{\left((W)^{0.5}\times\mathrm{Sin}\left(\frac{W}{C}\right)\times\mathrm{Sin}\left(\frac{S}{C}\right)\right)}\right]\times\left[\mathrm{Age}\times\mathrm{Ln}\left(\frac{W}{C}\right)\times\left(\mathrm{Ln}\left(\frac{S}{C}\right)+\sqrt[3]{\frac{Ms}{C}}\right)\right]^{2/9} \quad (6)$$

$$GEP_{Ff}-I=\frac{\left[\mathrm{Cos}\left(\mathrm{Arctan}\left(\frac{Ns}{C}\right)\right)+\frac{\mathrm{Cos}(86.086)}{\left(\frac{Ns}{C}-\frac{W}{C}\right)}\right]}{\mathrm{Cos}\left(\mathrm{Sin}\left(-5.01-\frac{S}{C}\right)\right)}\times\left(e^{\frac{Ms}{C}}\right)^{0.5}\times\left[\left[\mathrm{Cos}\left(\mathrm{Cos}\left(4.391+\frac{S}{C}\right)^{2}\times\mathrm{Arctan}\left(\frac{W}{C}+\frac{Ns}{C}\right)\right)\right]^{0.5}+\frac{Ms}{C}\right]\times\left[e^{\left[\mathrm{Cos}\left(\frac{4Ms\times Ns}{C^{2}}\right)\right]}+\left(\frac{Ns}{C}\right)^{1/9}\right] \quad (7)$$

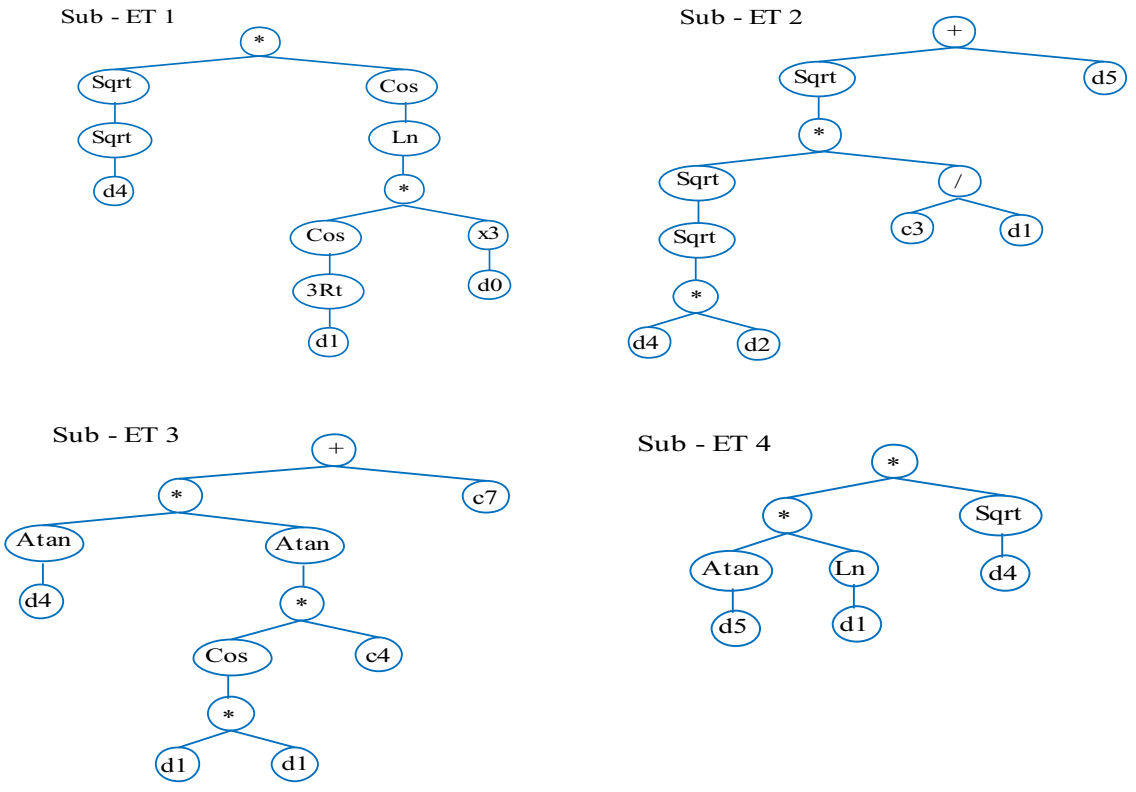

Fig. 13. Expression tree of GEPFc-I model.

All of the obtained results from the experimental and predicted studies using the training and testing results of GEP_{Fc}-I model at the age of 3, 7, 14, 21, and 28 days and GEP_{Ff}-I model at the age of 28 days are given in Figs. 14 and 15. The equation and R^2 of linear least square fit line had shown the training and testing values. The experimental results were compared with predicted training and testing results as shown in Figs. 14 and 15. There are two major parts in data series, which are related to training and testing data, including 0–130 and 130–160 series (compressive strength) and 0–26 and 26–32 series (flexural strength), respectively. It is clear that addition linking function has better performance than the multiplication approach of GEP-I in the training phase, while the R^2 values of GEP_{Fc}-I and GEP_{Ff}-I are equal to 0.9349 and 0.9280, respectively. As it can be seen from the Figs. 14 and 15, the training and testing values in GEP-I models, with both addition and multiplication approaches, have noticeable dispersion between the experimental and predicted results because of ignoring the porosity as the input parameter in GEP-I model.

6.2.2. Addition and multiplication models of GEP_{Fc}-II and GEP_{Ff}-II

Eqs. (8)–(11) show the mathematical non-linear formulation between input and output parameter for both addition and multiplication approaches (GEP_{Fc}-II and GEP_{Ff} -II) while the equations are obtained from trees. For example, Fig. 16 shows the ETs formulation of Eq. (8) for GEP_{Fc}-II.

$$\begin{aligned}GEP_{Fc}-II &= \mathrm{Age}+46.787+\left(\cos\left(\mathrm{Age}-\frac{Ns}{C}\right)\right)\\&+\mathrm{LnC}+\left(\mathrm{Cos}\left[\left(C^3\times 99.066\right)^2+14.167\times\left(-26.671+\frac{Ms}{C}\right)\right]^3\right)^{1/3}\\&+\left(\mathrm{Sin}\left(-86.427\times\frac{S}{C}\right)+4595.578\frac{Ns}{C}-\mathrm{Age}\right)^{1/3}\\&+\left(\left(173.877\times\frac{Ms}{C}\right)\times((60.044-\mathrm{Age})-(P+\mathrm{Age}))\right)^{1/3}-2P\end{aligned}\quad(8)$$

$$\begin{aligned}GEP_{Ff}-II &= \mathrm{Arc\,tan}\left[\mathrm{Ln}\left(\left(\frac{S}{C}-\frac{W}{C}\right)+Ns\right)-\left(\left(P\times\frac{W}{C}\right)^{0.5}-\mathrm{Sin}(P)\right)\right]\\&+\left[(\mathrm{Cos}(P)+72.53)^{1/3}+\left(\sqrt{25.891}-\mathrm{Sin}(P)\right)\right]\\&-\mathrm{Sin}\left(\frac{S}{C}\right)+\left[\frac{S}{C}-\left(\mathrm{Sin}(92.175)+44.844+\frac{P\times C}{W}\right)^{0.25}\right]^{1/3}\\&+\mathrm{Cos}\left[\mathrm{Cos}\left[\left(\sqrt{\frac{S}{C}}-\frac{Ns}{C}-46.613\right)-\left(\frac{Ms}{S}-C-5.313\right)\right]^2\right]\end{aligned}\quad(9)$$

$$\begin{aligned}GEP_{Fc}-II &= \left[\left(\left(45.498\times\mathrm{Age}\times\frac{Ns}{C}\times\frac{Ms}{C}\right)\right.\right.\\&\left.+\left(-49.537-\frac{Ns}{C}\right)\right)\times\sqrt{\mathrm{Ln}(P)}\Bigg]\times\frac{W}{C}\\&\times\mathrm{Cos}\left[\mathrm{Cos}\left(\mathrm{Arc\,tan}\left[\left(-55.906\times P\times\frac{Ns}{C}\right)\right.\right.\right.\\&\left.\left.\left.-\left(\frac{Ms}{C}-\frac{S}{C}\right)\times\mathrm{Sin}(-55.906)\right]\right)\right]\\&\times\frac{(\mathrm{Arc\,tan}(5.268-\mathrm{Age})+(\frac{S}{C}-23.148))\times\mathrm{Cos}^2(\frac{W}{C})}{P}\\&\times\left[\mathrm{Cos}\left(\mathrm{Sin}\frac{S}{C}\right)\right]^{1.5}\end{aligned}\quad(10)$$

$$\begin{aligned}GEP_{Ff}-II &= \left[\left(\mathrm{Cos}\frac{S}{C}\right)^3\times\left(68.502P+\mathrm{SinC}+\left(\frac{S}{C}-C\right)\right)^{1/3}\right]\\&\times e^{\left[\mathrm{Cos}\left(\mathrm{Cos}\left(\left(e^{-9.094}\right)^{1/3}-\mathrm{Sin}\left(\frac{Ns}{C}-\frac{S}{C}\right)\right)\right)\right]}\\&\times\left[\left(\left(\frac{(\frac{Ns}{C})^{1/3}}{C}\right)^{1/3}\times\mathrm{Arc\,tan}\frac{W}{C}\right)^{1/3}+\frac{W}{C}\right]^{1/3}\\&\times\mathrm{Cos}\left[\left(\frac{W}{C}\times\mathrm{Arc\,tan}\left[(\mathrm{Sin}(-85.328C))^2\right]\right)^3+\frac{W}{C}\right]\end{aligned}\quad(11)$$

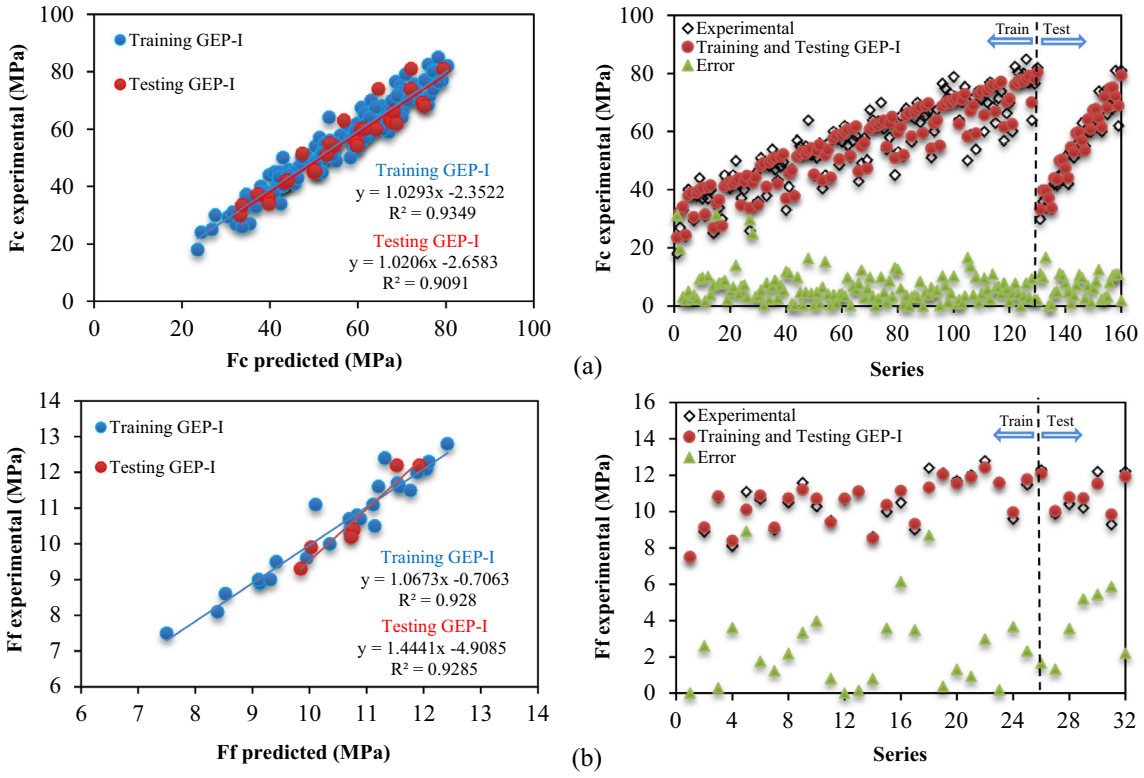

Fig. 14. Comparison and correlation of experimental results with predicted values of addition GEP-I approach model: (a) Compressive strength and (b) flexural strength.

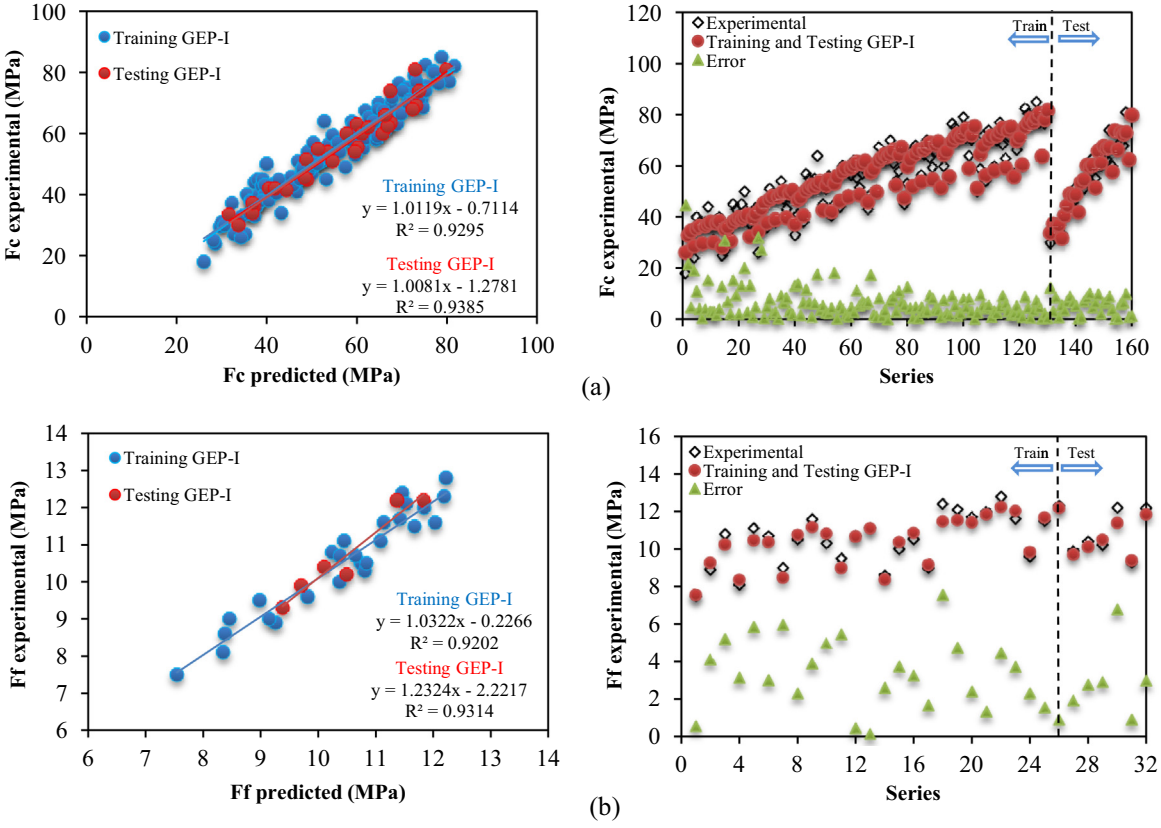

Fig. 15. Comparison and correlation of experimental results with predicted values of multiplication GEP-I approach model: (a) Compressive strength and (b) flexural strength.

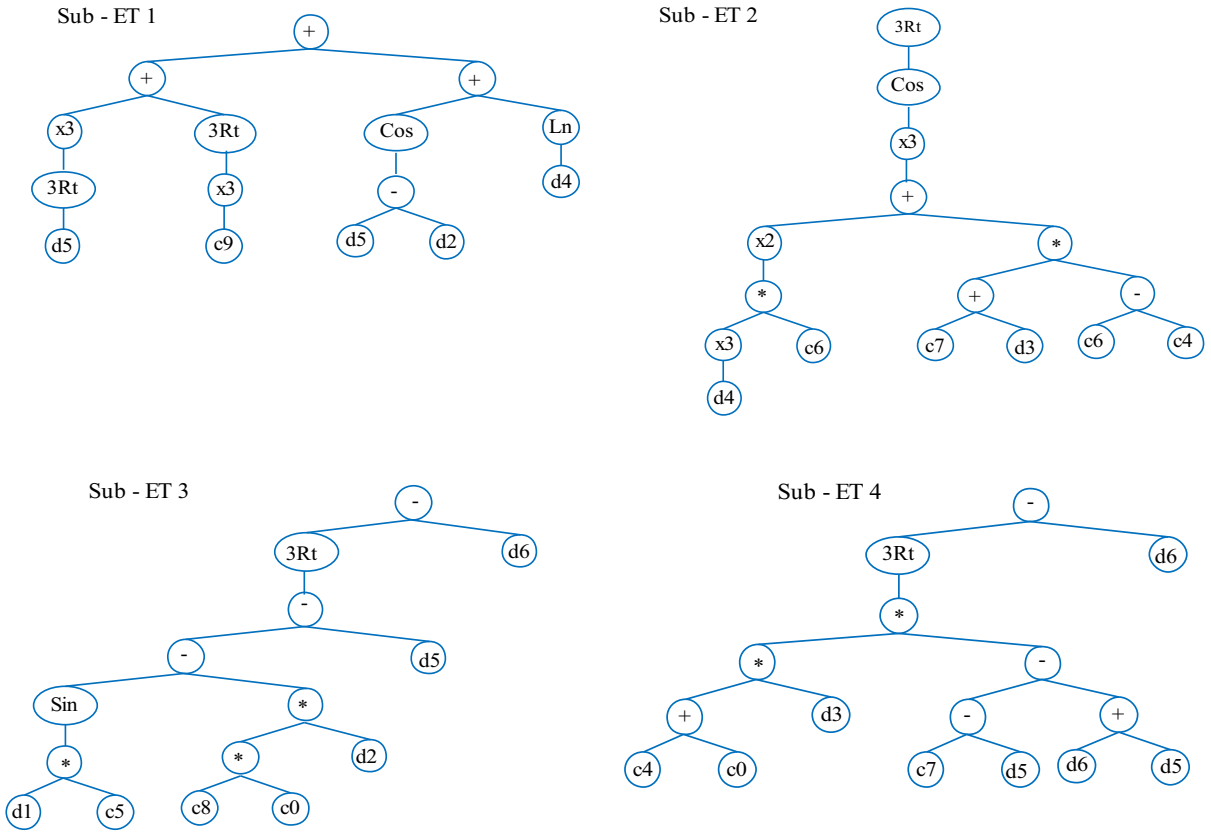

Fig. 16. Expression tree of GEPFc-II model.

Figs. 17 and 18 show the training and testing values in GEP-II model with both addition and multiplication approaches. The GEP-II models have the closest dispersion of experimental and predicted results, and also the training set result indicated that the non-linear relationship between input and output parameters was efficiently well learned with proposed models and it has the high correlation and approximately low error values because of considering porosity as input parameter. All of the models' results exhibit that addition linking function in GEP-II model has respectively the best performance among all GEP-II models with R^2 values of 0.9601 and 0.9452 for training compressive and flexural strength (GEP_{Fc}-II and GEP_{Ff}-II).

The statistical parameters' performance of the training and testing sets of the GEP-I and GEP-II with both addition and multiplication approach models are presented in Table 7. It shows that the best GEP models for predicting F_c and F_f is addition GEP-II model, because of the least error and the highest R^2 among both GEP-I and GEP-II models. The highest training value of R^2 and lowest values of MAPE and RMSE in the GEP_{Fc}-II (compressive strength) models are equal to 0.9601, 4.852, and 2.967, respectively, and also in the GEP_{Ff}-II (flexural strength) models, these values are equal to 0.9452, 2.483 and 0.3252, respectively.

All of the GEP models show that the suitable proposed model based on performance models and statistical values is addition GEP-II due to the fact that the effect of porosity is considered as the input parameter in mechanical properties of cement mortar.

The current study model compared with the previous literature models in terms of the selection of correct input parameters for predicting mechanical properties. In this regard, Deepa et al. [55], Erdal et al. [56], and Yeh and Lien [57] have used intelligence tools (ANN and GEP) for predicting the mechanical properties of cement-based materials. Nevertheless, the models didn't consider all effective input parameter such as porosity. The current study is proposed a new ANN and GEP model for predicting the strength properties of cement mortar which is containing Ns and Ms simultaneously. In fact, the simultaneous presence of small particles such as Ns and Ms create unique properties in cement mortar or concrete that considering them help to predict the properties of cement-based materials with all effective input parameters accurately. Table 8 provides a comparison review of some previous literature on strength properties prediction.

6.3. Verification of ANN and GEP proposed model

In order to evaluate the validation of ANN and GEP proposed model, the comparison process has been done with the last work of Jalal et al. [39], Said et al. [58] and Haruehansapong et al. [59], the collection data has been presented in appendix A. To achieve this purpose, the data sets were gathered from aforementioned studies and then applied in ANN and GEP current study, so current and collection data sets are considered as the input parameters and they are predicted by GEP-II and ANN-II proposed model as the best models. In these models, the current data was considered as training set, and the collection data weas considered as the testing set in order to validate the proposed models' performance. Figs. 19 and 20 show the validity and accuracy of the proposed ANN-II and GEP-II model in predicting compressive and flexural strengths with the help of a collection of collected data. Fig. 19 shows that the correlation coefficient values (R^2) of compressive and flexural ANN collected data are equal to 0.9396 and 0.9614, respectively. Also it shows the power of ANN proposed model to predict the result of the collected data due to high R^2. Fig. 20 illustrates the validation of GEP-II proposed model for both current and collected data. The compressive and flexural training R^2 values are equal to 0.9554 and 0.9429, respectively, and the compressive and flexural testing R^2 are equal to 0.9372 and 0.9689, respectively. Due to high R^2

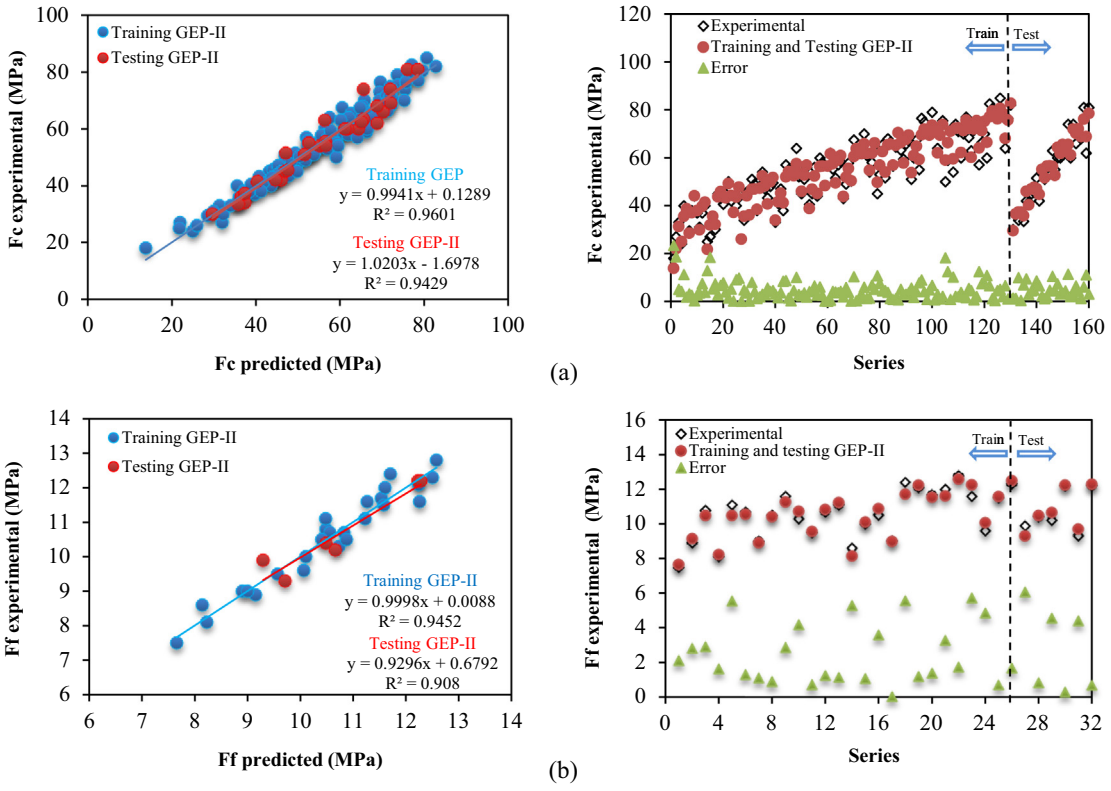

Fig. 17. Comparison and correlation of experimental results with predicted values of addition GEP-II approach model: (a) Compressive strength and (b) flexural strength.

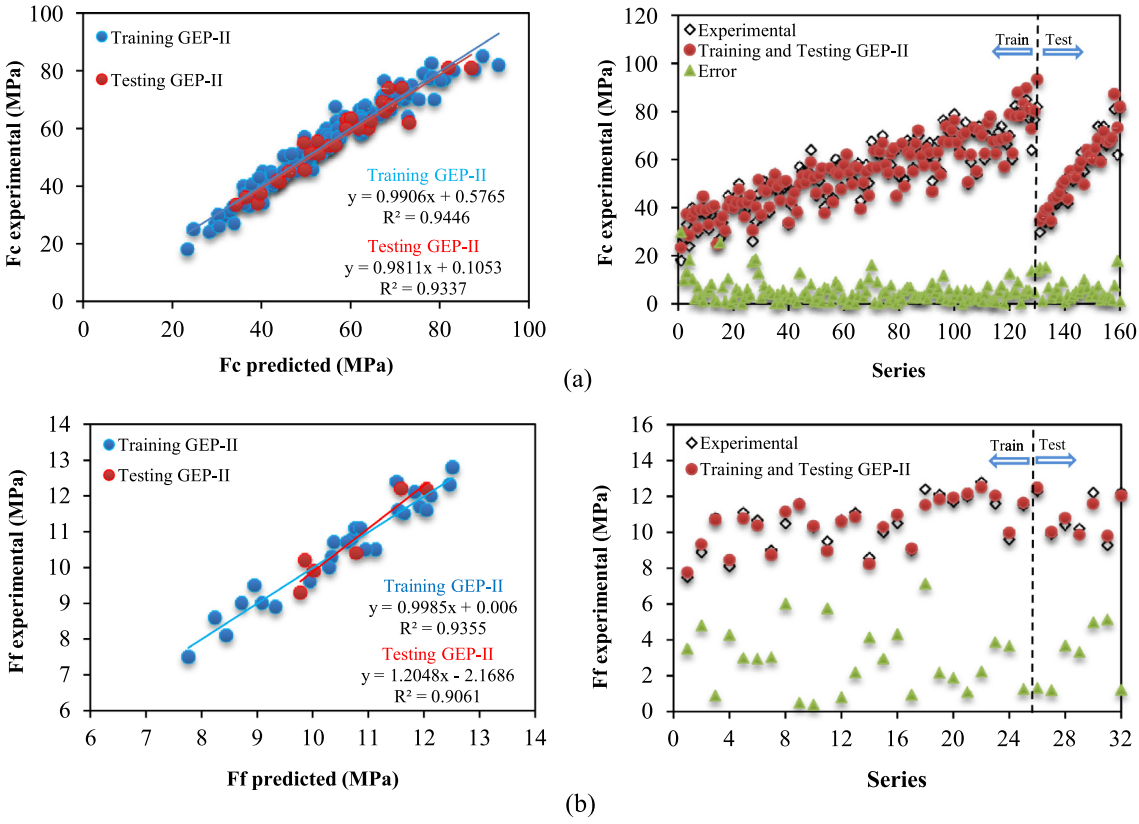

Fig. 18. Comparison and correlation of experimental results with predicted values of multiplication GEP-II approach model: (a) Compressive strength and (b) flexural strength.

Table 7
Statistical values of GEP-I and GEP-II models.

Approach	Model	R^2		MAPE		RMSE	
		Training	Testing	Training	Testing	Training	Testing
Addition	GEP_{Fc}-I	0.9349	0.9091	6.240	6.804	3.869	4.466
	GEP_{Ff}-I	0.9280	0.9285	2.516	3.952	0.3822	0.4575
Multiplication	GEP_{Fc}-I	0.9295	0.9385	6.404	5.423	3.935	3.554
	GEP_{Ff}-I	0.9202	0.9314	3.274	3.048	0.4095	0.4150
Addition	GEP_{Fc}-II	0.9601	0.9429	4.582	4.920	2.967	3.386
	GEP_{Ff}-II	0.9452	0.9080	2.483	2.806	0.3252	0.3562
Multiplication	GEP_{Fc}-II	0.9446	0.9337	5.177	5.450	3.488	3.612
	GEP_{Ff}-II	0.9355	0.9061	2.893	3.260	0.3530	0.3863

Table 8
Comparison of R^2 values for the current and previous ANN and GEP models.

Data Set	Method	R^2
Current study	ANN	0.9842
	GEP	0.9568
Deepa et al. [53]	ANN	0.6250
Erdal et al. [54]	ANN	0.9088
Yeh and Lien [55]	GEP	0.8669
	ANN	0.9338

values as shown in Fig. 20, the R^2 values of collection data show that the proposed GEP-II model has high accuracy to predict data. In fact, both ANN-II and GEP-II proposed models have suitable, reliable, and valid performance in the prediction compressive and flexural strengths of collected data.

Furthermore, a strong comparison procedure with the previous formulations has been done to validate the ANN and GEP proposed model. Smith [60] mentioned that the $R > 0.8$ has the appropriate correlation between experimental and predicted values. Frank and Todeschini [61] indicated that the minimum ratio of objects over the number of select variables is equal and>3 for model acceptability. This ratio for compressive and flexural data in current study are equal to 160/7 = 22.85 and 32/6 = 5.33, respectively. Golbraikh and Tropsha [62] suggested the method for verification of the GEP and ANN model based on one slope regression line (k or k′) close to 1; moreover, the m and n criteria performance must be lower than 0.1. Roy and Roy [63] offered performance indexes for external predicted models (R_m) in which the satisfied condition is at least 0.5. The squared correlation coefficient (Ro^2 or Ro'^2) should be close to 1 while Ro^2 is squared correlation coefficient between the predicted and experimental values, and Ro'^2 is squared correlation coefficient between experimental and predicted values [64]. The considered validation criteria of ANN-II and GEP-II model are presented in Table 9 for current and collection data. From the results, the proposed model is in accordance with the required conditions, and the validation phase strongly states that the proposed model is valid.

Consequently, this study presented proposed models to the prediction of the compressive and flexural strength of cement mortar, and it is well-known that cement mortar is as basic cementitious materials such a concrete that its characteristics can effect on

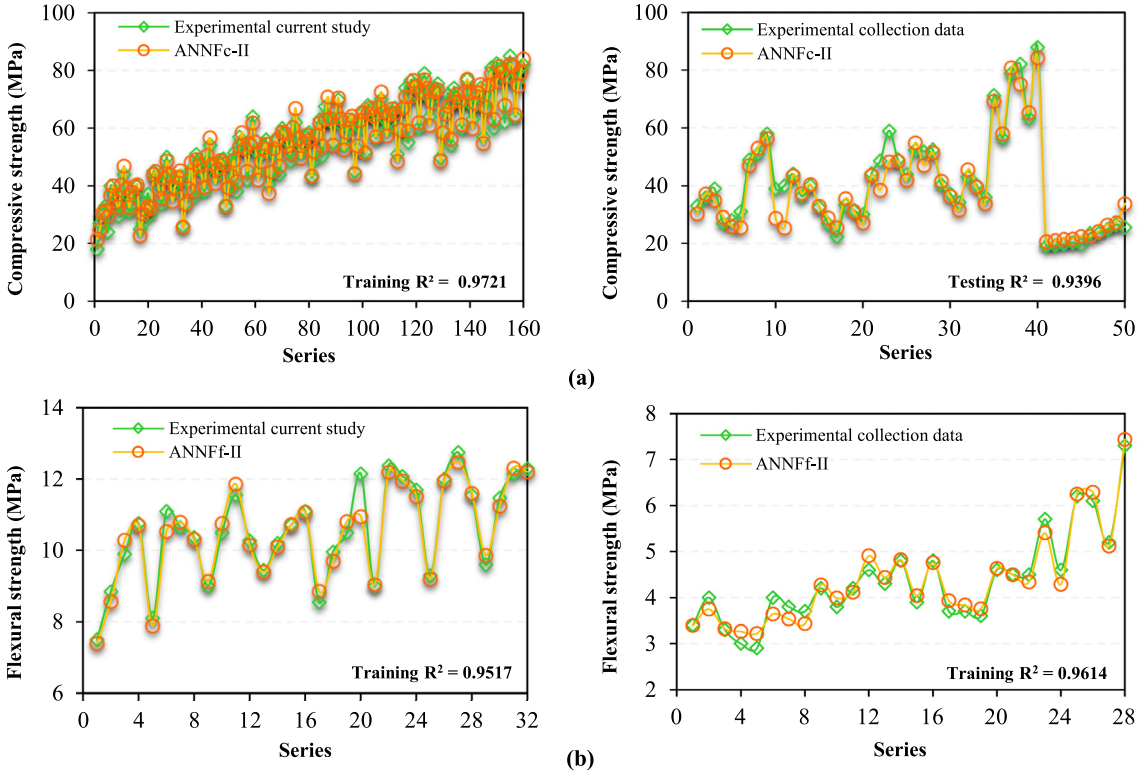

Fig. 19. Validation of proposed ANN-II model with data set collected: (a) Compressive strength and (b) flexural strength.

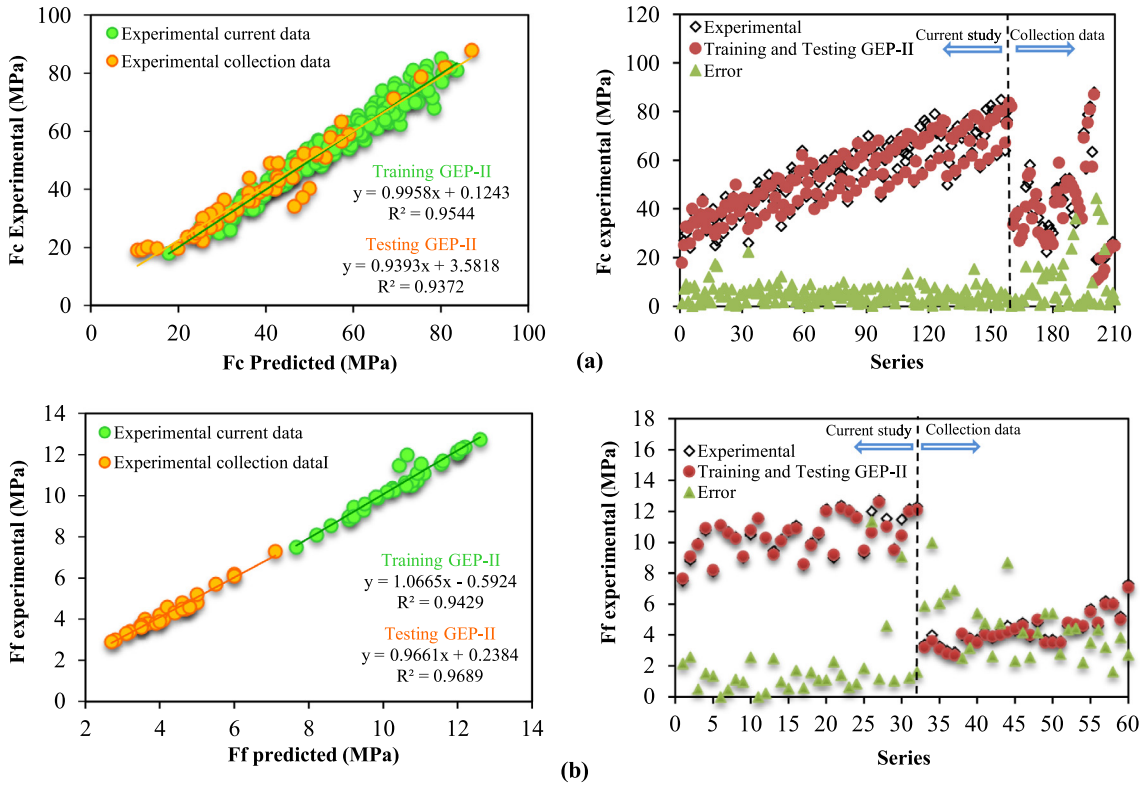

Fig. 20. Validation of proposed GEP-II model with data set collected: (a) Compressive strength and (b) flexural strength.

Table 9
Validation of ANN-II and GEP-II proposed model for current and collection data.

Item	Formula	Condition	Current study				Collection data			
			ANN-II		GEP-II		ANN-II		GEP-II	
			F_c	F_f	F_c	F_f	F_c	F_f	F_c	F_f
1	R	$R > 0.8$	0.9921	0.9846	0.9782	0.9669	0.9693	0.9805	0.9680	0.9843
2	$K = \frac{\sum_{i=1}^{n}(A_i \times P_i)}{\sum_{i=1}^{n} A_i^2}$	$0.85 < k < 1.15$	0.9966	0.9924	1.0017	1.0001	0.9672	1.0010	0.9742	0.9797
3	$K' = \frac{\sum_{i=1}^{n}(A_i \times P_i)}{\sum_{i=1}^{n} P_i^2}$	$0.85 < k' < 1.15$	1.0023	1.0071	0.9953	0.9989	1.0250	0.9972	1.0162	1.0189
4	$R_m = R^2 \times \left(1 - \sqrt{\lvert R^2 - Ro^2 \rvert}\right)$	$R_m > 0.5$	0.9143	0.7497	0.7608	0.6982	0.7371	0.7337	0.8640	0.6689
5	$m = \frac{R^2 - Ro^2}{R^2}$	$\lvert m \rvert < 0.1$	−0.0051	0.0530	−0.0438	−0.0698	−0.0494	−0.0396	−0.0065	0.0989
6	$n = \frac{R^2 - Ro'^2}{R^2}$	$\lvert n \rvert < 0.1$	−0.011	0.4030	−0.0369	−0.0683	−0.0568	−0.0137	−0.0428	0.0854
Where			0.9893	0.9182	0.9990	0.9989	0.9860	0.9994	0.9432	0.8730
$Ro^2 = 1 - \frac{\sum_{i=1}^{n}(P_i - A_i^o)^2}{\sum_{i=1}^{n}(P_i - P_i^o)^2}$, $A_i^o = k \times P_i$										
$Ro'^2 = 1 - \frac{\sum_{i=1}^{n}(A_i - P_i^o)^2}{\sum_{i=1}^{n}(A_i - A_i^o)^2}$, $P_i^o = k' \times A_i$			0.9951	0.9304	0.9924	0.9987	0.9930	0.9745	0.9773	0.8861

concrete properties. Hence, the proposed models can be extended to concrete materials. Furthermore, the effect of new materials in the model should be considered for the new cement-base materials.

7. Conclusion

In this study, an extensive experimental program including 32 mix designs in different percentages of Ns and Ms in form of alone (Ns or Ms) and together (Ns + Ms) was made for investigating the dependence of mechanical properties on each mix designs' porosity. In addition, the effect of porosity was evaluated to predict mechanical properties of cement mortar by ANN and GEP models. The following conclusions may be drawn based on the experimental and modeling results:

1) The addition of Ms and Ns has a significant effect on decreasing porosity and increasing the compressive and flexural strengths at different ages, while the porosity effect is higher at the age of 28 days specimens with lower W/B ratio, especially when Ns and Ms are combined together.
2) The optimum replacement dose of cement with Ns and Ms is obtained by 2.8% and 9% by weight of cement, respectively.
3) The presence of both Ns and Ms has the synergistic effect on microstructure, and it is perceived that the simultaneous use of Ns and Ms affected the densifying of cement mortar's microstructure.

4) Among cement mortar containing Ns and Ms, ANN and GEP are efficient for predicting the compressive and flexural strengths. Comparison between ANN and GEP models in terms of R^2, RMSE, and MAPE showed that ANN-II and GEP-II provide better results due to considering porosity as input parameter which is relative to the ANN-I and GEP-I modeling results.
5) The ANN model presents a more exact model based on the correlation coefficient and error rate relative to GEP model; instead, the GEP model provides a prediction formula based on the defined parameters.
6) Moreover, the validation of proposed models was investigated by collected data from previous literature. The validation results of the ANN-II and GEP-II models indicate the high accuracy of the proposed model.
7) Accordingly, the porosity is very significant and effective factor in the formation of mechanical properties, and also the effectiveness of porosity should be considered in the proposed models.

Declaration of Competing Interest

None.

Acknowledgment

The authors appreciate the support for this investigation by the central laboratory of Hakim Sabzevari University (member of network of Iranian science laboratories-NISL).

Appendix. A

Table A1.

Table A1
Data collection are used as validation sets.

Age (day)	W/C	C (Kg/m^3)	Aggregate (Kg/m^3)	Ns (Kg/m^3)	Ms (Kg/m^3)	F_c (MPa)	F_f (MPa)	Ref.
7	0.38	400	1581	0.00	0.00	36.40	3.40	[37]
7	0.38	500	1581	0.00	0.00	40.20	4.00	[37]
7	0.40	380	1581	0.00	0.00	32.70	3.30	[37]
7	0.42	360	1581	0.00	0.00	26.90	3.00	[37]
7	0.45	340	1581	0.00	0.00	22.40	2.90	[37]
7	0.40	475	1581	0.00	0.00	33.20	4.00	[37]
7	0.42	450	1581	0.00	0.00	31.50	3.80	[37]
7	0.45	425	1581	0.00	0.00	30.10	3.70	[37]
7	0.39	392	1581	8.00	0.00	44.30	4.20	[37]
7	0.42	360	1581	0.00	40.00	48.70	3.80	[37]
7	0.43	352	1581	8.00	40.00	59.00	4.20	[37]
7	0.39	490	1581	10.00	0.00	49.10	4.60	[37]
7	0.42	450	1581	0.00	50.00	43.90	4.30	[37]
7	0.43	440	1581	10.00	50.00	52.30	4.80	[37]
28	0.38	400	1581	0.00	0.00	51.80	3.90	[37]
28	0.38	500	1581	0.00	0.00	52.50	4.80	[37]
28	0.40	380	1581	0.00	0.00	40.40	3.70	[37]
28	0.42	360	1581	0.00	0.00	37.30	3.70	[37]
28	0.45	340	1581	0.00	0.00	34.20	3.60	[37]
28	0.40	475	1581	0.00	0.00	43.10	4.60	[37]
28	0.42	450	1581	0.00	0.00	40.30	4.50	[37]
28	0.45	425	1581	0.00	0.00	36.10	4.50	[37]
28	0.39	392	1581	8.00	0.00	71.30	5.70	[37]
28	0.42	360	1581	0.00	40.00	56.50	4.60	[37]
28	0.43	352	1581	8.00	40.00	78.80	6.20	[37]
28	0.39	490	1581	10.00	0.00	82.10	6.10	[37]
28	0.42	450	1581	0.00	50.00	63.40	5.20	[37]
28	0.43	440	1581	10.00	50.00	87.90	7.30	[37]
3	0.40	390	1973	0.00	0.00	33.00	–	[56]
3	0.37	390	1958	23.40	0.00	36.00	–	[56]
3	0.37	390	1936	46.80	0.00	39.00	–	[56]
3	0.57	273	1938	0.00	0.00	27.00	–	[56]
3	0.53	273	1923	23.40	0.00	28.00	–	[56]
3	0.49	273	1905	46.80	0.00	31.00	–	[56]
7	0.40	390	1973	0.00	0.00	49.00	–	[56]
7	0.37	390	1958	23.40	0.00	51.00	–	[56]
7	0.37	390	1936	46.80	0.00	58.00	–	[56]
7	0.57	273	1938	0.00	0.00	39.00	–	[56]
7	0.53	273	1923	23.40	0.00	40.00	–	[56]
7	0.49	273	1905	46.80	0.00	44.00	–	[56]
7	0.65	0.800	2.2	0.00	0.00	19.16	–	[57]
7	0.67	0.776	2.2	0.00	0.02	19.27	–	[57]
7	0.69	0.752	2.2	0.00	0.05	19.69	–	[57]
7	0.70	0.746	2.2	0.00	0.05	20.24	–	[57]
7	0.74	0.704	2.2	0.00	0.10	19.64	–	[57]
28	0.65	0.800	2.2	0.00	0.00	23.52	–	[57]
28	0.67	0.776	2.2	0.02	0.00	23.67	–	[57]
28	0.69	0.752	2.2	0.05	0.00	24.92	–	[57]
28	0.70	0.746	2.2	0.05	0.00	26.46	–	[57]
28	0.74	0.704	2.2	0.10	0.00	25.61	–	[57]

W = Water, C = Cement, Ns = Nano silica, Ms = Micro silica, Fc = Compressive strength and Ff = Flexural strength.

References

[1] V. Afroughsabet, L. Biolzi, P.J. Monteiro, The effect of steel and polypropylene fibers on the chloride diffusivity and drying shrinkage of high-strength concrete, Compos. B Eng. 139 (2018) 84–96.
[2] H. Eskandari, Designing, proposing and comparing the methods predicting the compressive strength of the ferro cement mortar, Concr. Res. Lett. 6 (1) (2015) 1–10.
[3] H. Eskandari, A. Madadi, Investigation of ferrocement channels using experimental and finite element analysis, Eng. Sci. Technol., Int. J. 18 (4) (2015) 769–775.
[4] X. Chen, S. Wu, Influence of water-to-cement ratio and curing period on pore structure of cement mortar, Constr. Build. Mater. 38 (2013) 804–812.
[5] V.G. Haach, G. Vasconcelos, P.B. Lourenço, Influence of aggregates grading and water/cement ratio in workability and hardened properties of mortars, Constr. Build. Mater. 25 (6) (2011) 2980–2987.
[6] S. Mahdinia, H. Eskandari-Naddaf, R. Shadnia, Effect of cement strength class on the prediction of compressive strength of cement mortar using GEP method, Constr. Build. Mater. 198 (2019) 27–41.
[7] G.A. Rao, Development of strength with age of mortars containing silica fume, Cem. Concr. Res. 31 (8) (2001) 1141–1146.
[8] A. Kooshkaki, H. Eskandari-Naddaf, Effect of porosity on predicting compressive and flexural strength of cement mortar containing micro and nano-silica by multi-objective ANN modeling, Constr. Build. Mater. 212 (2019) 176–191.
[9] S. Pandey, R. Sharma, The influence of mineral additives on the strength and porosity of OPC mortar, Cem. Concr. Res. 30 (1) (2000) 19–23.
[10] A. Ghanei, H. Eskandari-Naddaf, A. Davoodi, Corrosion behavior and optimization of air-entrained reinforced concrete, incorporating microsilica, Struct. Concr. 19 (5) (2018) 1472–1480.
[11] Y.-Y. Kim, K.-M. Lee, J.-W. Bang, S.-J. Kwon, Effect of W/C ratio on durability and porosity in cement mortar with constant cement amount, Adv. Mater. Sci. Eng. 2014 (2014).
[12] H. Eskandari-Naddaf, R. Kazemi, Experimental evaluation of the effect of mix design ratios on compressive strength of cement mortars containing cement strength class 42.5 and 52.5 MPa, Procedia Manuf. 22 (2018) 392–398.
[13] S. Fallah, M. Nematzadeh, Mechanical properties and durability of high-strength concrete containing macro-polymeric and polypropylene fibers with nano-silica and silica fume, Constr. Build. Mater. 132 (2017) 170–187.
[14] L. Zapata, G. Portela, O. Suárez, O. Carrasquillo, Rheological performance and compressive strength of superplasticized cementitious mixtures with micro/nano-SiO2 additions, Constr. Build. Mater. 41 (2013) 708–716.
[15] M. Azimi-Pour, H. Eskandari-Naddaf, ANN and GEP prediction for simultaneous effect of nano and micro silica on the compressive and flexural strength of cement mortar, Constr. Build. Mater. 189 (2018) 978–992.
[16] Y. Su, J. Li, C. Wu, P. Wu, Z.-X. Li, Influences of nano-particles on dynamic strength of ultra-high performance concrete, Compos. B Eng. 91 (2016) 595–609.
[17] M. Stefanidou, I. Papayianni, Influence of nano-SiO2 on the Portland cement pastes, Compos. B Eng. 43 (6) (2012) 2706–2710.
[18] M. Lezgy-Nazargah, S. Emamian, E. Aghasizadeh, M. Khani, Predicting the mechanical properties of ordinary concrete and nano-silica concrete using micromechanical methods, Sādhanā 43 (12) (2018) 196.
[19] B. Sabir, Mechanical properties and frost resistance of silica fume concrete, Cem. Concr. Compos. 19 (4) (1997) 285–294.
[20] L. Li, Z. Huang, J. Zhu, A. Kwan, H. Chen, Synergistic effects of micro-silica and nano-silica on strength and microstructure of mortar, Constr. Build. Mater. 140 (2017) 229–238.
[21] L. Li, J. Zhu, Z. Huang, A. Kwan, L. Li, Combined effects of micro-silica and nano-silica on durability of mortar, Constr. Build. Mater. 157 (2017) 337–347.
[22] H. Li, H.-G. Xiao, J. Yuan, J. Ou, Microstructure of cement mortar with nano-particles, Compos. B Eng. 35 (2) (2004) 185–189.
[23] A.U. Ozturk, B. Baradan, A comparison study of porosity and compressive strength mathematical models with image analysis, Comput. Mater. Sci. 43 (4) (2008) 974–979.
[24] T. Korouzhdeh, H. Eskandari-Naddaf, M. Gharouni-Nik, An improved ant colony model for cost optimization of composite beams, Appl. Artif. Intell. 31 (1) (2017) 44–63.
[25] S. Akkurt, S. Ozdemir, G. Tayfur, B. Akyol, The use of GA–ANNs in the modelling of compressive strength of cement mortar, Cem. Concr. Res. 33 (7) (2003) 973–979.
[26] H. Adeli, Neural networks in civil engineering: 1989–2000, Comput.-Aided Civ. Infrastruct. Eng. 16 (2) (2001) 126–142.
[27] D.E. Goldberg, M.P. Samtani, Engineering optimization via genetic algorithm, Electronic computation, ASCE, 1986, pp. 471–482.
[28] H. Eskandari-Naddaf, R. Kazemi, ANN prediction of cement mortar compressive strength, influence of cement strength class, Constr. Build. Mater. 138 (2017) 1–11.
[29] M. Ghaemi-Fard, H. Eskandari-Naddaf, G.R. Ebrahimi, Genetic prediction of cement mortar mechanical properties with different cement strength class after freezing and thawing cycles, Struct. Concr. 19 (5) (2018) 1341–1352.
[30] Z. Yuan, L.-N. Wang, X. Ji, Prediction of concrete compressive strength: Research on hybrid models genetic based algorithms and ANFIS, Adv. Eng. Softw. 67 (2014) 156–163.
[31] S. Gupta, Using artificial neural network to predict the compressive strength of concrete containing Nano-Silica, Civ. Eng. Archit. 1 (3) (2013) 96–102.
[32] C. Astm, 778: Standard specification for standard sand, Annual Book of ASTM Standards 4 (2006).
[33] M.S. Meddah, A. Tagnit-Hamou, Pore structure of concrete with mineral admixtures and its effect on self-desiccation shrinkage, Mater. J. 106 (3) (2009) 241–250.
[34] S. Kamali, B. Gérard, M. Moranville, Modelling the leaching kinetics of cement-based materials––influence of materials and environment, Cem. Concr. Compos. 25 (4–5) (2003) 451–458.
[35] K. Haga, S. Sutou, M. Hironaga, S. Tanaka, S. Nagasaki, Effects of porosity on leaching of Ca from hardened ordinary Portland cement paste, Cem. Concr. Res. 35 (9) (2005) 1764–1775.
[36] Md. Safiuddin, Nataliya Hearn, Comparison of ASTM saturation techniques for measuring the permeable porosity of concrete, Cement and Concrete Research 35 (5) (2005) 1008–1013.
[37] C. Qian, M. Ba, X. Guo, X. Han, Evaluation of sub-microstructure in concrete with low water-binder ratio by SEM-BSE image analysis, Journal of Wuhan University of Technology-Mater, Sci. Ed. 25 (4) (2010) 682–686.
[38] J. Massana, E. Reyes, J. Bernal, N. León, E. Sánchez-Espinosa, Influence of nano- and micro-silica additions on the durability of a high-performance self-compacting concrete, Constr. Build. Mater. 165 (2018) 93–103.
[39] M. Jalal, A. Pouladkhan, O.F. Harandi, D. Jafari, Comparative study on effects of Class F fly ash, nano silica and silica fume on properties of high performance self compacting concrete, Constr. Build. Mater. 94 (2015) 90–104.
[40] Y. Qing, Z. Zenan, K. Deyu, C. Rongshen, Influence of nano-SiO2 addition on properties of hardened cement paste as compared with silica fume, Constr. Build. Mater. 21 (3) (2007) 539–545.
[41] R. Yu, P. Spiesz, H. Brouwers, Effect of nano-silica on the hydration and microstructure development of Ultra-High Performance Concrete (UHPC) with a low binder amount, Constr. Build. Mater. 65 (2014) 140–150.
[42] T. Ji, Preliminary study on the water permeability and microstructure of concrete incorporating nano-SiO2, Cem. Concr. Res. 35 (10) (2005) 1943–1947.
[43] S.-C. Lee, Prediction of concrete strength using artificial neural networks, Eng. Struct. 25 (7) (2003) 849–857.
[44] M.N. Hadi, Neural networks applications in concrete structures, Comput. Struct. 81 (6) (2003) 373–381.
[45] A. NeuroIntelligence, Alyuda NeuroIntelligence Manual, 2010.
[46] B.R. Prasad, H. Eskandari, B.V. Reddy, Prediction of compressive strength of SCC and HPC with high volume fly ash using ANN, Constr. Build. Mater. 23 (1) (2009) 117–128.
[47] J.H. Holland, Genetic algorithms, Sci. Am. 267 (1) (1992) 66–73.
[48] J.R. Koza, Genetic programming: on the programming of computers by means of natural selection, MIT press1992.
[49] M. Sonebi, A. Cevik, Genetic programming based formulation for fresh and hardened properties of self-compacting concrete containing pulverised fuel ash, Constr. Build. Mater. 23 (7) (2009) 2614–2622.
[50] K. Haghdar, H. Shayanfar, M.S. Alavi, Selective Harmonics Elimination of Multi Level Inverters via Methods of GPS, SA and GA, Power and Energy Engineering Conference (APPEEC), IEEE, 2011, Asia-Pacific, 2011. 1-5.
[51] C. Ferreira, Gene expression programming: mathematical modeling by an artificial intelligence, Springer, 2006.
[52] C. Ferreira, U. Gepsoft, What is gene expression programming, 2008.
[53] T. USED, Gene Expression Programming:-A New Adaptive Algorithm for Solving Problems.
[54] G. Gepsoft, Version 5.0, 2014
[55] C. Deepa, K. SathiyaKumari, V.P. Sudha, Prediction of the compressive strength of high performance concrete mix using tree based modeling, Int. J. Comput. App. 6 (5) (2010) 18–24.
[56] H.I. Erdal, O. Karakurt, E. Namli, High performance concrete compressive strength forecasting using ensemble models based on discrete wavelet transform, Eng. Appl. Artif. Intell. 26 (4) (2013) 1246–1254.
[57] I.-C. Yeh, L.-C. Lien, Knowledge discovery of concrete material using genetic operation trees, Expert Syst. Appl. 36 (3) (2009) 5807–5812.
[58] A.M. Said, M.S. Zeidan, M. Bassuoni, Y. Tian, Properties of concrete incorporating nano-silica, Constr. Build. Mater. 36 (2012) 838–844.
[59] S. Haruehansapong, T. Pulngern, S. Chucheepsakul, Effect of the particle size of nanosilica on the compressive strength and the optimum replacement content of cement mortar containing nano-SiO2, Constr. Build. Mater. 50 (2014) 471–477.
[60] G.N. Smith, Probability and statistics in civil engineering, Collins Professional and Technical Books 244 (1986).
[61] I.E. Frank, R. Todeschini, The data analysis handbook, Elsevier, 1994.
[62] A. Golbraikh, A. Tropsha, Beware of q2!, J Mol. Graph. Model. 20 (4) (2002) 269–276.
[63] P.P. Roy, K. Roy, On some aspects of variable selection for partial least squares regression models, Mol. Inf. 27 (3) (2008) 302–313.
[64] A.H. Alavi, M. Ameri, A.H. Gandomi, M.R. Mirzahosseini, Formulation of flow number of asphalt mixes using a hybrid computational method, Constr. Build. Mater. 25 (3) (2011) 1338–1355.